Life Sciences 232 (2019) 116620

Contents lists available at ScienceDirect

Life Sciences

journal homepage: www.elsevier.com/locate/lifescie

Pacemaker cell characteristics of differentiated and *HCN4*-transduced human mesenchymal stem cells

Fabrice F. Darche[a], Rasmus Rivinius[a], Eva Köllensperger[b], Uwe Leimer[b], Günter Germann[b], Anja Seckinger[c], Dirk Hose[c], Julian Schröter[a], Claus Bruehl[d], Andreas Draguhn[d], Richard Gabriel[e], Manfred Schmidt[e], Michael Koenen[a,f], Dierk Thomas[a,g], Hugo A. Katus[a,g], Patrick A. Schweizer[a,g,*]

[a] Department of Cardiology, Medical University Hospital Heidelberg, INF 410, D-69120 Heidelberg, Germany
[b] ETHIANUM Klinik Heidelberg, Voßstraße 6, D-69115 Heidelberg, Germany
[c] Department of Hematology, Oncology and Rheumatology, Medical University Hospital Heidelberg, INF 410, D-69120 Heidelberg, Germany
[d] Institute for Physiology and Pathophysiology, University of Heidelberg, INF 326, D-69120 Heidelberg, Germany
[e] Molecular and Gene Therapy, National Center for Tumor Diseases (NCT) Heidelberg, INF 460, D-69120 Heidelberg, Germany
[f] Department of Molecular Neurobiology, Max-Planck-Institute for Medical Research, Jahnstrasse 29, D-69120 Heidelberg, Germany
[g] DZHK (German Centre for Cardiovascular Research), partner site Heidelberg/Mannheim, University of Heidelberg, INF 410, D-69120 Heidelberg, Germany

ARTICLE INFO

Keywords:
Biological pacemaker
Mesenchymal stem cells
Ion channels
Electrophysiology
Differentiation

ABSTRACT

Aims: Cell-based biological pacemakers aim to overcome limitations and side effects of electronic pacemaker devices. We here developed and tested different approaches to achieve nodal-type differentiation using human adipose- and bone marrow-derived mesenchymal stem cells (haMSC, hbMSC).

Main methods: haMSC and hbMSC were differentiated using customized protocols. Quantitative RT-PCR was applied for transcriptional pacemaker-gene profiling. Protein membrane expression was analyzed by immunocytochemistry. Pacemaker current (I_f) was studied in haMSC with and without lentiviral HCN4-transduction using patch clamp recordings. Functional characteristics were evaluated by co-culturing with neonatal rat ventricular myocytes (NRVM).

Key findings: Culture media-based differentiation for two weeks generated cells with abundant transcription of ion channel genes (*Ca_v1.2*, *NCX1*), transcription factors (*TBX3*, *TBX18*, *SHOX2*) and connexins (*Cx31.9* and *Cx45*) characteristic for cardiac pacemaker tissue, but lack adequate *HCN* transcription. haMSC-derived cells revealed transcript levels, which were closer related to sinoatrial nodal cells than hbMSC-derived cells. To substitute for the lack of I_f, we performed lentiviral *HCN4*-transduction of haMSC resulting in stable I_f. Co-culturing with NRVM demonstrated that differentiated haMSC expressing *HCN4* showed earlier onset of spontaneous contractions and higher beating regularity, synchrony and rate compared to co-cultures with non-*HCN4*-transduced haMSC or *HCN4*-transduced, non-differentiated haMSC. Confocal imaging indicated increased membrane expression of cardiac gap junctional proteins in differentiated haMSC.

Significance: By differentiation haMSC, rather than hbMSC attain properties favorable for cardiac pacemaking. In combination with lentiviral *HCN4*-transduction, a cellular phenotype was generated that sustainably controls and stabilizes rate in co-culture with NRVM.

1. Introduction

Pacemaker activity controlling cardiac excitation is elicited by specialized cells located in a restricted area of the heart, termed the sinoatrial node (SAN). SAN cells, among other features, are characterized by abundant expression of the hyperpolarization-activated and cyclic nucleotide-gated ion channel HCN4 [1] that underlies the funny current (I_f), a key factor for the generation of regular sinus rhythm [2–7]. Currently, electronic pacemakers are the only effective therapy for symptomatic bradycardia. However, technical limitations such as battery durability, difficulties in the placement of the stimulating electrode, electrode dysfunction, infection, and the lack of response to the autonomic modulatory system are major disadvantages [8,9]. With respect to these shortcomings, biological pacemakers may better adapt

* Corresponding author at: Department of Cardiology, University of Heidelberg, INF 410, D-69120 Heidelberg, Germany.
E-mail address: patrick.schweizer@med.uni-heidelberg.de (P.A. Schweizer).

https://doi.org/10.1016/j.lfs.2019.116620
Received 8 March 2019; Received in revised form 21 June 2019; Accepted 29 June 2019
Available online 07 July 2019

to the physiological requirements of the patient [10].

Promising strategies to achieve biological pacemaking include the use of stem cells to substitute loss of native pacemaker cells [11] or the implementation of genes via plasmids or viral vectors to initiate spontaneous activity of formerly quiescent cardiomyocytes [9,12]. However, cellular approaches (i.e. pluripotent stem cells of fetal cardiomyocytes) were confined by the risk of immune rejection, immaturity or lack of cellular transdifferentiation, whereas gene therapy is limited by only transient effects and systemic infection harboring oncological or arrhythmogenic safety issues.

Previously, both strategies were combined in a hybrid proof of concept approach using mesenchymal stem cells (MSC) as vehicle for targeted gene transfer of pacemaker ion channels to the heart. To this end, MSC were transfected in vitro using *HCN2* or *HCN4* gene transfer and injected into the subepicardium of large animals [13,14] to successfully generate pacemaker activity in vivo. However, pacemaking was restricted to a time period of several weeks, possibly due to a loss of transplanted cells that did not stay at the sites of injection and/or the use of nucleofection or non-integrating viral vectors and consecutive loss-of-function of target gene. This suggests that native adult stem cells may not durably integrate within cardiac tissue and with decreasing activity of pacemaker gene constructs may not be sufficient to facilitate spontaneous heartbeat. However, despite various "proof-of-concept" studies investigating the applicability of MSC to establish gene-transfer-mediated biological pacemaker activity in vivo [13,14], none of these studies have investigated the differentiation potential and the cellular and molecular properties of modified MSC to attain pacemaker cell properties.

We here explored and compared various approaches to achieve pacemaker-type cell differentiation of human MSC, derived from adipose tissue (haMSC) and bone-marrow (hbMSC). Moreover, differentiated/non-differentiated haMSC were subjected to lentiviral *HCN4* gene transfer to improve pacemaker cell properties. The different approaches were evaluated on a molecular and functional level to investigate the utility and limitations of MSC to achieve a cellular pacemaker phenotype.

2. Material and methods

2.1. Mesenchymal stem cell isolation and culture

Human mesenchymal stem cells (hMSC) were obtained from adipose tissue (haMSC) isolated by abdominal plastic surgery and from bone marrow (hbMSC). Frozen vials of pre-characterized hbMSCs isolated from bone marrow aspirates of healthy donors were obtained from the Center for the Preparation and Distribution of Adult Stem Cells (Institute for Regenerative Medicine, Texas A&M College of Medicine, College Station, TX, USA; NIH/NCRR grant P40 RR 17447–06). Protocols of hMSC isolation and handling were approved by the local ethical committee (University of Heidelberg ethical committee number: S-462 / 2010). haMSC and hbMSC originated from 3 different donors each (haMSC donors 1–3; hbMSC donors 4–6), and were isolated according to standard protocols and expanded in hMSC expansion medium [15]. hMSC expansion medium consisted of 58% Dulbecco's modified Eagle medium (DMEM) low glucose (Thermo Fisher Scientific, Waltham, Massachusetts, USA), 40% MCDB 201 (Sigma-Aldrich, St. Louis, Missouri, USA), 2% fetale bovine serum (FBS, Thermo Fisher Scientific), 100 U/ml penicillin (Thermo Fisher Scientific), 100 µg/ml streptomycin (Thermo Fisher Scientific), 2 mM L-Glutamine (Thermo Fisher Scientific), 1× Insulin-Transferrin-Selenium (ITS) (Thermo Fisher Scientific), 1× Linoleic Acid-Albumin (Sigma-Aldrich), 10^{-4} M L-Ascorbic acid (Sigma-Aldrich), 10 µg/ml human recombinant platelet-derived growth factor-BB (PDGF-BB, Peprotech, Rocky Hill, New Jersey, USA), 10 µg/ml human recombinant endothelial growth factor (EGF, Peprotech) und 5 mM dexamethasone (Sigma-Aldrich).

haMSC and hbMSC cultures used in this study were passaged 5 times, achieving 70–80% confluency. The characterization of native haMSC (for nearer details, see Supplementary Materials) and hbMSC was determined by their cluster of differentiation (CD) marker profile and their ability to differentiate into osteogenic, adipogenic, and chondrogenic lineages as previously reported [16,17].

2.2. Culture-media based differentiation assays

For differentiation, haMSC and hbMSC were grown for 2 weeks each, using five different culture-media: 1. hMSC expansion media, 2. hMSC expansion medium +10 ng/ml human recombinant BMP4, 3. hMSC expansion medium +100 ng/ml human recombinant activin A, 4. RPMI-1640 + B27 supplement (Thermo Fisher Scientific, Waltham, Massachusetts, USA) + 10 ng/ml human recombinant BMP4 (Peprotech, Rocky Hill, New Jersey, USA), 5. RPMI-1640 + B27 supplement +100 ng/ml human recombinant activin A (Peprotech). The differentiation assays using RPMI-1640 + B27 supplement were related to a protocol for cardiac differentiation of human embryonic stem cells, as previously described [18]. All differentiation experiments were performed in triplicate, and repeated at least twice.

2.3. hHCN4-IRES-eGFP vector construction

Vector construction was performed using standard cloning procedures [19,20]. Briefly, a multiple cloning site (BamHI-BstB1-Sbf1-Bcl1-*Asi*SI-*Bst*Z17I-*Psp*XI) was introduced into the unique BamH1 site of lentiviral plasmid construct pCCLsin.cPPT.SFFV.IRES.eGFP.WPRE (kindly provided by Prof. Luigi Naldini, Italy). Subsequently, the SFFV promotor [21] was replaced by a CMV promotor using the restriction-enzymes *Cla*I and BamH1 to generate pCCLsin.cPPT.CMV.MCS.IRES.eGFP.WPRE. Human *HCN4* cDNA was cloned into cytomegalovirus promotor directed expression vectors [5]. *Bst*BI and *Asi*SI restriction sites were introduced 5′ and 3′ of the *HCN4* coding region, and used to introduce *HCN4* into pCCLsin.cPPT.CMV.MCS.IRES.eGFP.WPRE to obtain pCCLsin.cPPT.CMV.hHCN4.IRES.eGFP.WPRE.

GFP expression from the EMCV internal ribosomal entry site (IRES) [22,23] was used to visualize successfully transduced cells by their fluorescence signal that also allowed accumulation of HCN4 expressing cells by FACS sorting (FACSCalibur, Becton Dickinson Biosciences, Franklin Lakes, New Jersey, USA). Finally, we generated the lentiviral vector CMV.hHCN4.IRES.eGFP.

2.4. Generation of lentiviral particles

VSV-pseudotyped, self-inactivating, third-generation vectors were produced by transient transfection of 293 T cells using packaging plasmids (PlasmidFactory, Bielefeld, Germany), and Polyethylenimine (Sigma-Aldrich, St. Louis, Missouri, USA) and viral particles were concentrated by ultra-centrifugation as previously described [19,20] with the following modifications:

A total of 1×10^7 293 T cells were seeded in 20 × 15-cm-diameter dishes 24 h prior to transfection in modified IMDM (Thermo Fisher Scientific) with 10% fetal bovine serum (FBS, Thermo Fisher Scientific), 2 mM penicillin/streptomycin (Thermo Fisher Scientific) and 2 mM glutamine (Thermo Fisher Scientific) in a 5% CO_2 incubator. Culture medium was changed 2 h prior to transfection. A total of 28 µg of transgene vector (*HCN4*-construct), 12.5 µg of LV 101 (3rd Generation Gag/Pol-Packaging plasmid), 6.25 µg of LV102 (pRSV-rev plasmid) and 9 µg of LV 103 (VSV-G) per dish were added to 5 ml IMDM. Additionally, 167.25 µg of PEI per dish were added to this solution and mixed well. After 30 min of incubation at room temperature, transfection mix was drop-wise applied to cells which were then incubated for 12–14 h at 37 °*C. Medium* (15 ml) was replaced after 12 to 14 h; the viral supernatant was collected after another 24 h, filtered through 0.22-mm-pore-size filters, and isolated by ultracentrifuge (SW-28 rotor at 20000 rpm, room temperature for 2 h). Viral pellets were resolved in

PBS and samples of 10, 20 and 50 µl were frozen and stored at −80 °C. To determine the titer of the viral solution, 5×10^4 HeLa cells were cultured per well (6-well-plate) in DMEM (Thermo Fisher Scientific) 10% FBS (PAN), 2 mM penicillin/streptomycin (Thermo Fisher Scientific) and 2 mM glutamine (Thermo Fisher Scientific) and incubated for 24 h at 37 °C and 5% CO_2. The next day, medium was changed and a 10-fold dilution series of the viral vector stock was generated (10^{-3} to 10^{-7}) in the presence of 8 µg/ml Polybrene (Sigma-Aldrich). Cells were transduced, incubated at 37 °C and 5% CO_2 for further 72 h, and then harvested using standard protocol [19,20]. GFP expression was evaluated by FACS analysis. Lentiviral particles without HCN4-construct were produced in parallel as control.

2.5. Lentiviral HCN4-transduction of haMSC

Overexpression of HCN4 in native human mesenchymal stem cells from adipose tissue (nhaMSC) (donor 3) was performed by lentiviral transduction. To this end, 100,000 nhaMSC (donor 3) per well were seeded on 6-well plates, previously coated with 0.1 mg/ml fibronectin (Roche Diagnostics, Rotkreuz, Switzerland) / phosphate buffered saline (PBS, Thermo Fisher Scientific) solution and infected with 1 million lentiviruses carrying human *HCN4* in 300 µl of hMSC expansion medium. 24 h after infection, 700 µl of hMSC expansion medium were added to the cells. hMSC medium change was performed 24 h later. 72–96 h after infection, cells were visualized by an Olympus IX 70 fluorescence microscope (Olympus, Tokyo, Japan) in order to determine the amount of GFP-positive cells. To obtain a pure culture of *HCN4*-transduced nhaMSC (nhaMSC-HCN4$^+$) (donor 3), GFP-positive cells were sorted by a BD Facial Action Coding System (FACS) Aria II (Becton Dickinson Biosciences, Franklin Lakes, New Jersey, USA). Subsequently, parts of the sorted cells were cultured in differentiation medium for 2 weeks. Differentiated and *HCN4*-transduced cells were designated dhaMSC-HCN4$^+$ (donor 3). As control, nhaMSC were transduced with lentiviral particles lacking *HCN4*-construct using the protocol described above, designated as dhaMSC-HCN4$^-$ (donor 3).

2.6. RNA preparation

Total ribonucleic acid (RNA) was isolated using Trizol® reagent (Thermo Fisher Scientific) following the manufactor's instructions. Human adult RNA of the right atrium (hRA) was purchased from Biocat (BioCat GmbH, Heidelberg, Germany).

2.7. Copy DNA synthesis

For reverse transcription, 10 mM deoxynucleotide trisphosphates (dNTP) (Thermo Fisher Scientific) and 250 ng Random Primers (Thermo Fisher Scientific) were added to 3 µg of total RNA and incubated for 5 min at 65 °C. Afterwards, 40 U of RNAse Out (Thermo Fisher Scientific), 5× First Strand Buffer (Thermo Fisher Scientific), 100 mM DTT (Thermo Fisher Scientific) and 200 U Superscript II Reverse Transcriptase (Thermo Fisher Scientific) were added. The mixture was incubated for 10 min at room temperature followed by an incubation of 1 h at 42 °C.

2.8. Quantitative real-time

Quantification was performed using a 7500 real-time polymerase chain reaction (PCR) system (Thermo Fisher Scientific) and 96 well optical detection plates (Thermo Fisher Scientific). Wells were loaded to a total volume of 10 µl consisting of 40 ng copy deoxyribonucleic acid (cDNA), 1× TaqMan Universal Master Mix (Thermo Fisher Scientific) and pre-designed TaqMan probes and primers (TaqMan Gene Expression Assays, Thermo Fisher Scientific) specific to human *TBX3*, *TBX18*, *SHOX2*, *BMP4*, *GATA4*, *MEF2C*, *NKX2.5*, *cTnI*, *HCN1*, *HCN2*, *HCN4*, *NCX1*, *Ca_v1.2*, *Ca_v1.3*, *Ca_v3.1*, *SCN5A*, *Cx31.9*, *Cx45*, *Cx40*, *Cx43*, *α_{1a}-adrenergic receptor*, *β_1-adrenergic receptor*, *β_2-adrenergic receptor*, *CHRM2*, *K_{ir}2.1*, *hERG* and *K_v4.3* as well as the housekeeping genes *GAPDH*, *HPRT1* and *ACTB* used for normalization. Table S1 lists the protein and the corresponding genetic names of the used primers. Probes were labeled with the fluorescent reporter dye ROX (ROX, Thermo Fisher Scientific) at the 5′ end and with the non-fluorescent quencher at the 3′ end. Cycling conditions comprised an initial denaturing step at 95 °C (10 min) and 40 cycles with 95 °C (15 s) and 60 °C (40 s). All PCR reactions were performed in triplicate and data are expressed as an average of the triplicates.

Data were analyzed using the threshold cycle (CT) relative quantification method as published elsewhere [24,25]. We calculated target gene expression relative to a normalized reference, consisting of a subset of housekeeping genes including *GAPDH*, *HPRT1* and *ACTB*, as published elsewhere [26]. To evaluate relative abundance of gene expression compared to human pacemaker tissue, we analyzed abundance of gene transcripts in human right atrial tissue. Using specified right atrium/sinoatrial node (RA/SAN) transcriptional relations, as published previously [1], we calculated the putative amount of human SAN transcripts, as original human SAN tissue was inaccessible.

2.9. Immunocytochemistry

For immunocytochemistry, coverslips with 12 mm of diameter were coated with 10 ng/ml fibronectin solution. After an incubation for at least 30 min at 37 °C, fibronectin solution was aspirated and 2×10^4 cells of native and differentiated hMSC from adipose tissue and bone marrow as well as native and differentiated *HCN4*-transduced hMSC from adipose tissue were each seeded on coverslips. In co-culture assays, 6×10^3 haMSC were cultivated on fibronectin-coated coverslips and after 24 h 1.4×10^4 NRVM were added. The next day, respectively after 5 days of co-culture, cells were rinsed with PBS and fixed for 15 min in 1% formaldehyde (Merck Millipore, Burlington, Massachusetts, USA)/PBS solution at room temperature. After three washes with PBS, cells were incubated for 15 min in 0.5% Triton X-100/PBS solution at room temperature for membrane permeabilization. Afterwards they were washed in PBS and incubated for 1 h in 0.1 M glycine (Merck Millipore)/PBS solution at room temperature. They were then blocked for half an hour in 2% Bovine Serum Albumin (BSA) (Sigma-Aldrich) / PBS solution. Primary antibodies were incubated overnight in 2% BSA/PBS at 4 °C: anti-HCN1 (IgG, rabbit, Alomone Labs, Jerusalem, Israel) diluted 1:200, anti-HCN2 (IgG, rabbit, Alomone Labs) diluted 1: 200, anti-HCN4 (IgG, rabbit, Alomone Labs) diluted 1: 200, anti-Ca_v1.2 (IgG, mouse, abcam, Cambridge, United Kingdom) diluted 1: 100, anti-Cx31.9 (IgG, rabbit, Santa Cruz Biotechnology, Dallas, Texas, United States) diluted 1: 200, anti-Cx43 (IgG, rabbit, Santa Cruz Biotechnology) diluted 1:200 and anti-Cx45 (IgG, rabbit, Santa Cruz Biotechnology) diluted 1:200. For co-culture experiments, cells were incubated with anti-HCN4 (IgG, rabbit, Alomone Labs) diluted 1:200. The next day, cells were washed with PBS (3 × 2 min) and incubated with secondary antibodies in 2% BSA/PBS at 4 °C for 4 h: MFP555 goat anti-rabbit IgG (H + L) (MoBiTec GmbH, Gottingen, Germany) diluted 1: 200 and MFP488 goat anti-mouse IgG 1 (H + L) (MoBiTec GmbH) diluted 1: 200. In co-culture assays, nuclei were counterstained with 1 µg/ml 4′,6-diamidino-2-phenylindole (DAPI, Sigma-Aldrich, St. Louis, Missouri, USA) for 30 min. After 3 washes with PBS, cells were mounted in Citifluor Glycerol/PBS Solution (Agar Scientific, Stansted, UK) and analyzed using a Leica SP2 AOBS (Leica Microsystems, Wetzlar, Germany, http://www.leica.com) confocal microscope. For each cell line, 20 cells were analyzed. The membrane expression was classified according to the classification: undetectable 0, weak 1, medium 2, strong 3, very strong 4. The images were edited using Adobe Photoshop (Adobe Systems Incorporated, San Jose, California, USA) and ImageJ software (National Institutes of Health, Bethesda, Maryland, United States).

Table 1
Ion channels and transporters relevant to cardiac pacemaking.

	nhaMSC donors				nhbMSC donors			dhaMSC donors				dhbMSC donors		
	1	2	3	3-HCN4$^+$	1	2	3	1	2	3	3-HCN4$^+$	1	2	3
TBX3	−	+	−	−	−	−	−	+	+	+	+	−	−	−
HCN1	−	−	−	−	−	−	−	−	+	−	+	+	−	−
HCN2	+	+	+	+	+	+	+	+	+	+	+	+	+	+
HCN4	−	−	−	+	−	−	−	−	−	−	+	−	−	−
NCX1	−	−	−		−	−	−	−	−	−		−	−	−
$Ca_v1.2$	+	−	−		−	−	−	+	+	+		+	−	−
$Ca_v1.3$	−	−	−		−	−	−	+	−	+		−	−	−
$Ca_v3.1$	−	−	−		−	−	−	+	−	+		+	−	−
Cx31.9	+	+	−		−	−	−	+	+	+		+	−	+
Cx45	−	−	−	−	−	−	−	+	−	−	+	−	+	−
α_{1a}-AR	−	−	−		−	−	−	+	+	+		−	+	−
β_1-AR	−	−	−	+	−	−	−	−	−	−	+	−	−	−
β_2-AR	−	−	−	−	−	−	−	+	−	+	+	+	+	−
CHMR2	−	−	−		−	−	−	+	−	+		−	−	+
Sum	3/14	3/14	1/14 (1/7)	3/7	1/14	1/14	1/14	10/14	6/14	9/14 (3/7)	7/7	6/14	4/14	3/14

+ denotes ≥70% of transcript levels related to the hSAN; − indicates < 70% transcript levels related to the hSAN. The sum is the number of genes with ≥70% of transcript levels related to the hSAN compared to the total number of analyzed genes. Except for *HCN4*-transduced native and differentiated haMSC donor 3, where 7 genes were determined, 14 genes were analyzed for each cell group. Moreover, same 7 genes as in *HCN4*-transduced native and differentiated haMSC donor 3 were also analyzed in non-transduced native and differentiated haMSC donor 3. The concerned sum is put into brackets.

2.10. I_f recording using patch-clamp electrophysiology

nhaMSC, dhaMSC and dhaMSC-HCN4$^+$, all of donor 3 (2×10^4 cells, each) were seeded on fibronectin-coated coverslips. The following day, I_f was recorded by whole-cell patch-clamp technique using an Axopatch 200B amplifier (Molecular Devices, San Jose, CA, USA). The pipette solution was composed of 10 mM NaCl (Merck Millipore, Billerica, MA, USA), 130 mM KCl (Merck Millipore), 0.5 mM $MgCl_2$ (Merck Millipore), 1 mM EGTA (Merck, Darmstadt, Germany), 5 mM HEPES (Merck), 2 mM Mg-ATP (Merck), 0.1 mM Na-GTP (Merck) and 5 mM phosphocreatine (Merck). pH was adjusted to 7.4 by KOH (Merck Millipore). The bath solution contained 30 mM KCl, 110 mM NaCl, 1.8 mM $CaCl_2$ (Merck Millipore), 0.5 mM $MgCl_2$ and 5 mM HEPES. pH was adjusted to 7.4 by NaOH. The osmolarities of the pipette and bath solution were adjusted to 290 (pipette solution) and 300 (bath solution) mOsmol/l, respectively, by adding appropiate amounts of glucose (Merck Millipore). Recordings were performed on 7 cells of each group (nhaMSC, dhaMSC and dhaMSC-HCN4$^+$, all of donor 3). To evaluate cAMP responsiveness of I_f, 10 µM cAMP (Merck) was added to the pipette solution. I_f recordings were carried out as previously described [5]. For the activation protocol, voltage steps from −40 to −140 mV were applied. Current amplitudes and time constants were plotted against corresponding voltage steps. Recordings were evaluated using Signal Software (Version 4.05, CED, Cambridge, UK). Calculations were performed in Excel 2010 (Microsoft, Redmond, WA, USA). Graphic illustrations were processed using Origin 7G (OriginLab, Northampton, MA, United States) and Draw X4 (Corel, Ottawa, Canada).

2.11. Co-culture of human MSC with neonatal rat ventricular myocytes

Ventricular myocytes derived from 1 day-old neonatal rats (NRVM) (Crl:Wls River, strain code 003, coat colour white, Charles River, Wilmington, Massachusetts, USA) were prepared as previously reported [27]. Protocols were approved by the local regulatory authority (T-38/14, Regierungspräsidium Karlsruhe, Germany). NRVM were cultured in Medium 199 (Sigma-Aldrich) supplemented with 5 ml 10^5 UI penicillin, 5 ml 10^5 µg/ml streptomycin and 10% fetal bovine serum at 37 °C in a 95% air/5% CO_2 humidified atmosphere for 2–3 days.

Native or differentiated haMSC with or without lentiviral *HCN4*-transduction were cultured on 35 mm dishes (ibidi GmbH, Planegg, Germany) at a number of 200,000. 24 h later, 2,000,000 NRVM were added to each dish. Dishes with 2,000,000 NRVM monolayer, served as baseline control. Beating rate, synchrony and regularity of each dish were determined from day 0 to day 9 for each group (10 dishes). To evaluate mean beating rate, the arithmetic mean and SEM from day 1 to day 7 was calculated. At day 4, cells were stimulated with 1 µM isoproterenol to study for chronotropic response.

2.12. Analysis of intracellular calcium transients and beating rate variability

To detect spontaneous calcium spikes in NRVM, cells were loaded with 10 µM Ca^{2+}-sensitive fluorescent indicator fluo-4-AM dissolved in buffer (in mM: 137 NaCl, 5.4 KCl, 1.8 $CaCl_2$, 0.5 $MgCl_2$, 10 HEPES, 5.5 glucose, pH 7.4) incubated for 10 min at 37 °C. Fluorescence signals were visualized using a confocal microscopy (Olympus FluoView1000). Fluo-4 was excited at 473 nm and emission was collected above 500 nm. Temporal resolution was 10 µs per pixel. Data were analyzed in OriginPro (OriginLab, Northampton, MA, USA). To assess the beating rate variability of the different cultures, Poincaré plot analysis was carried for NRVM, NRVM + nhaMSC, NRVM + dhaMSC, NRVM + nhaMSC-HCN4$^+$ and NRVM + dhaMSC-HCN4$^+$. Standard deviation of the long term R-R interval (SD1) and of the short term R-R interval (SD2) was evaluated, as previously described [28]. Each experiment was performed in triplicate.

2.13. Statistical analysis

All experiments and primary analyses were blinded. Statistical analysis was performed using GraphPad Prism (Version 6.0, GraphPad Software, Inc., San Diego, CA, USA). Transcript levels of each group of samples from a donor source ($n = 6$) was characterized by calculating the arithmetic means as well as the standard error of the mean (SEM). Comparison of transcriptional levels between multiple groups was performed using one-way ANOVA followed by a Tukey posthoc test. Pairwise comparison was performed by two-tailed unpaired Student's *t*-test. Differences were considered significant at a level $p < 0.05$. In order to quantitatively assess pacemaker gene transcription, we compared levels to approximated levels of the hSAN [1]. Transcription was judged as similar to hSAN (marked as positive in Table 1), when levels for a particular gene were at least 70% of hSAN levels. SD1 and SD2 values of each culture were characterized by calculating the arithmetic means as well as the standard error (SD). Comparison of SD1 and SD2 among cultures was performed using one-way ANOVA followed by a

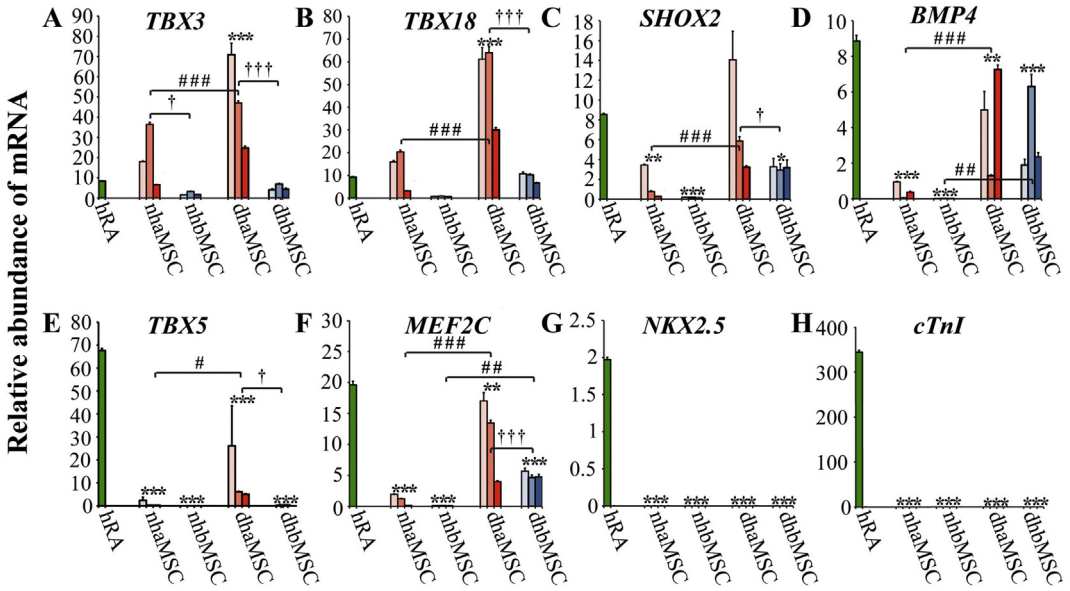

Fig. 1. Transcription profiling of pacemaker- and myocardium-specific transcriptional regulators and markers.
Relative abundance of mRNA transcription, analyzed by qRT-PCR. A-D, SAN-related transcription factors; *E*-G, myocardium-related transcription factors; H, myocardial marker troponin I. hRA = human right atrium (dark green); nhaMSC = native human mesenchymal stem cells from adipose tissue: pink = donor 1, light red = donor 2, red = donor 3; nhbMSC = native human mesenchymal stem cells from bone marrow: light blue = donor 4, blue = donor 5, dark blue = donor 6; dhaMSC = differentiated human mesenchymal stem cells from adipose tissue: pink = donor 1, light red = donor 2, red = donor 3; dhbMSC = differentiated human mesenchymal stem cells from bone marrow: light blue = donor 4, blue = donor 5, dark blue = donor 6. Statistical significance - compared to hRA is indicated by *, − of nhaMSC / nhbMSC vs. dhaMSC / dhbMSC is denoted by #, − of nhaMSC / dhaMSC vs. nhbMSC / dhbMSC is marked by †. Data are provided as mean ± SEM. */#/† $p < 0.05$, **/##/†† $p < 0.01$, ***/###/††† $p < 0.001$. Comparison between multiple groups was performed using one-way ANOVA followed by a Tukey posthoc test. (For interpretation of the references to colour in this figure legend, the reader is referred to the web version of this article.)

Tukey posthoc test. Differences were considered significant at a level $p < 0.05$.

3. Results

3.1. Culture-media based differentiation of human mesenchymal stem cells derived from adipose tissue (haMSC) and bone marrow (hbMSC)

We first tested the utility of cell-culture media based differentiation of haMSC and hbMSC to achieve pacemaker-type transcription profiles. Total RNA of haMSC and hbMSC, which were cultured for 2 weeks according to the different protocols, were isolated and after reverse transcription, used for quantitative polymerase chain reaction (PCR) profiling of pacemaker-related genes. Our data indicated that RPMI medium supplemented with B27 and human bone morphogenetic protein 4 (BMP4) (10 ng/ml) most efficiently enhanced the transcription of genes involved in cardiac pacemaking (Figs. 1 and 2). Results of our additional approaches for pacemaker cell differentiation are depicted in the Supplementary material (Fig. S3).

3.1.1. Nodal- and working-type transcription factors

T-box transcription factors (TBX) 3 and 18 contribute importantly to the development of the human pacemaker and conduction system by suppression of chamber differentiation [29] and activation of nodal-specific genetic pathways [30]. Both are expressed in native haMSC, but only to a minor extent in hbMSC. Differentiation significantly increased transcription of *TBX3* (2.3-fold, $p < 0.001$) and *TBX18* (3.9-fold higher, $p < 0.001$) in dhaMSC to levels clearly above RA levels and similar to levels previously published for the hSAN [1]. In dhbMSC, in contrast, gene expression remained low (Fig. 1, A, B). Other transcription factors that have been associated with SAN development are short stature homeobox 2 (SHOX2) and its direct target BMP4 [31]. Both were transcribed moderately in native haMSC / hbMSC with slightly higher levels in haMSC, but markedly increased upon differentiation (Fig. 1, C, D). A different and more heterogenous pattern appeared for transcription factors TBX5, MEF2C and NKX2.5 known to regulate "working-type" cardiomyocyte differentiation. *TBX5* was barely transcribed in native hMSC (Fig. 1, E), but increased significantly upon differentiation in dhaMSC (12.1-fold, $p < 0.05$), although values still ranged below hRA levels (Fig. 1, E). In differentiated hbMSC, in contrast, levels remained low (Fig. 1, E). *MEF2C* was weakly transcribed in haMSC and almost absent from hbMSC. Differentiation increased *MEF2C* levels moderately in both haMSC and hbMSC (Fig. 1, F). By contrast, transcription factor *NKX2.5* was neither detectable nor inducible by our differentiation approach in haMSC as well as in hbMSC, (Fig. 1, G).

3.1.2. Cardiac structure protein

Minor level of cardiac troponin I *(cTnI)* were detected in native hMSC and despite 10-fold upregulation through differentiation remained very low compared to hRA levels (Fig. 1, H).

3.1.3. Ion channels and transporters

Hyperpolarization-activated cyclic nucleotide channels (HCN) produce I_f, importantly involved in SAN pacemaker activity [6,7]. *HCN1* is abundantly expressed in the SAN [32,33], but transcripts were hardly detectable in native hMSC. In differentiated haMSC, however, transcription increased markedly reaching levels comparable to the hSAN [1] (156-fold increase, $p < 0.001$) (Fig. 2, A). Interestingly, *HCN2* is highly transcribed in native haMSC and hbMSC similar to published hSAN levels [1] and differentiation resulted in even higher levels (Fig. 2, B) in both cell types. Transcripts of *HCN4*, most importantly contributing to I_f in the hSAN, were almost absent from native and differentiated haMSC and hbMSC (Fig. 2, C). Sodium-calcium exchanger (*NCX1*) levels were low in haMSC and hbMSC, but increased by differentiation (dhaMSC 2-fold increase; dhbMSC 4-fold increase, $p < 0.001$) (Fig. 2, D), still being significantly lower than in the hSAN [1] or hRA. Although present in hMSC, transcripts of L-type calcium

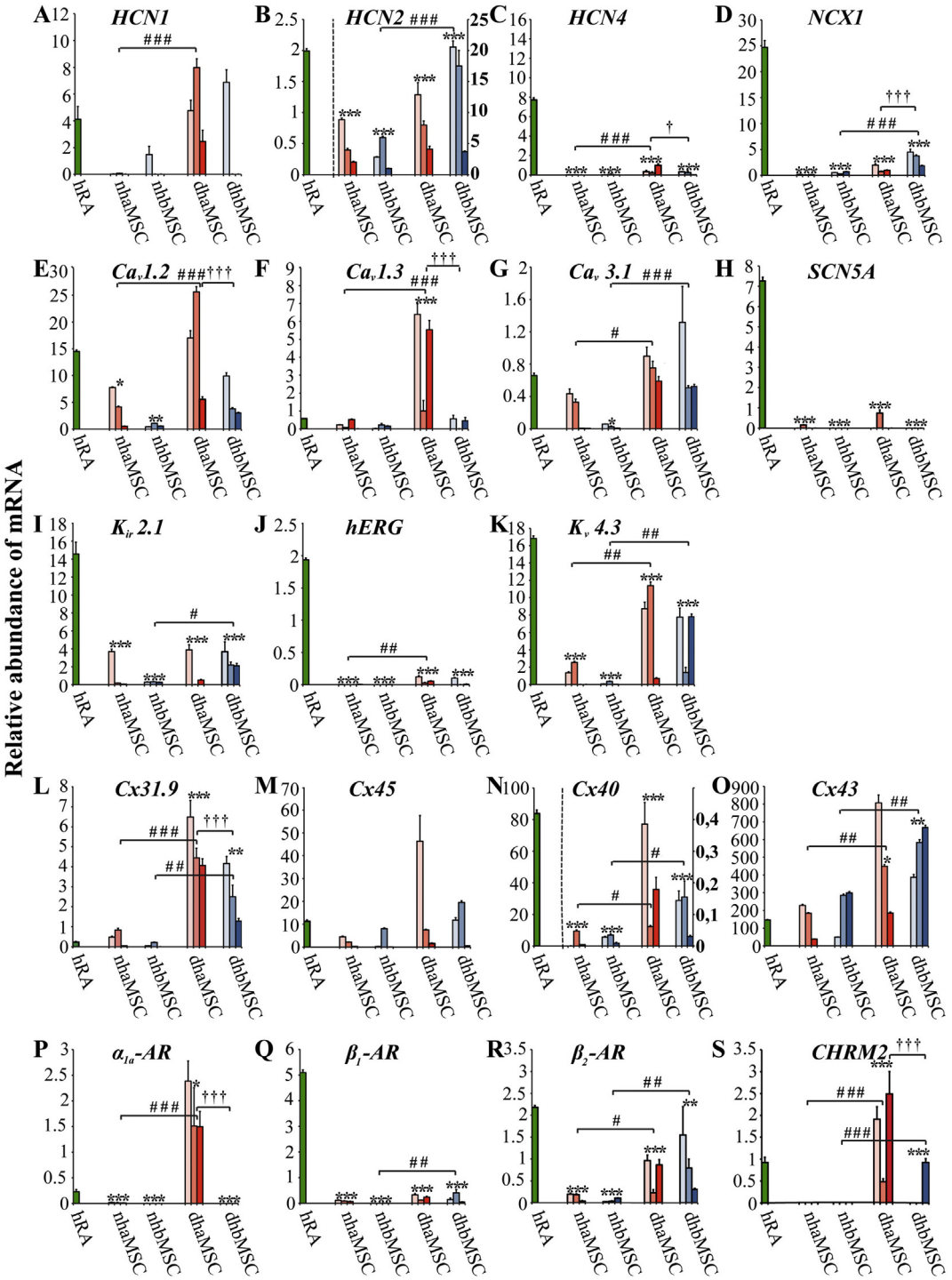

Fig. 2. Transcription profiling of ion channels, transporters, connexins and adrenergic receptors.
Relative abundance of mRNA transcription, analyzed by qRT-PCR. A-C, *HCN* channels; D, Na-Ca exchanger *NCX1*; E-G, calcium channels; H, sodium channel *SCN5A*; I-K, potassium channels; L-O, connexins; P-S, adrenergic and cholinergic receptors. hRA = human right atrium (dark green); nhaMSC = native human mesenchymal stem cells from adipose tissue: pink = donor 1, light red = donor 2, red = donor 3; nhbMSC = native human mesenchymal stem cells from bone marrow: light blue = donor 4, blue = donor 5, dark blue = donor 6; dhaMSC = differentiated human mesenchymal stem cells from adipose tissue: pink = donor 1, light red = donor 2, red = donor 3; dhbMSC = differentiated human mesenchymal stem cells from bone marrow: light blue = donor 4, blue = donor 5, dark blue = donor 6. Statistical significance - compared to hRA is indicated by *, − of nhaMSC / nhbMSC vs. dhaMSC/dhbMSC is denoted by #, − of nhaMSC / dhaMSC vs. nhbMSC / dhbMSC is marked by †. Data are provided as mean ± SEM. */#/† $p < 0.05$, **/##/†† $p < 0.01$, ***/###/††† $p < 0.001$. Comparison between multiple groups was performed using one-way ANOVA followed by a Tukey posthoc test. (For interpretation of the references to colour in this figure legend, the reader is referred to the web version of this article.)

channel subunits *$Ca_v1.2$* and *$Ca_v1.3$* and T-type subunit *$Ca_v3.1$* were low (Fig. 2, E-G). Differentiation resulted in marked upregulation of *$Ca_v1.2$* and *$Ca_v1.3$* in dhaMSC (3.9-fold increase, $p < 0.05$ and 15.3-fold increase, $p < 0.001$, respectively) with gene expression levels higher than those published for the hSAN [1] (Fig. 2, E, F). In hbMSC, however, transcription of *$Ca_v1.2$* and *$Ca_v1.3$* increased only moderately

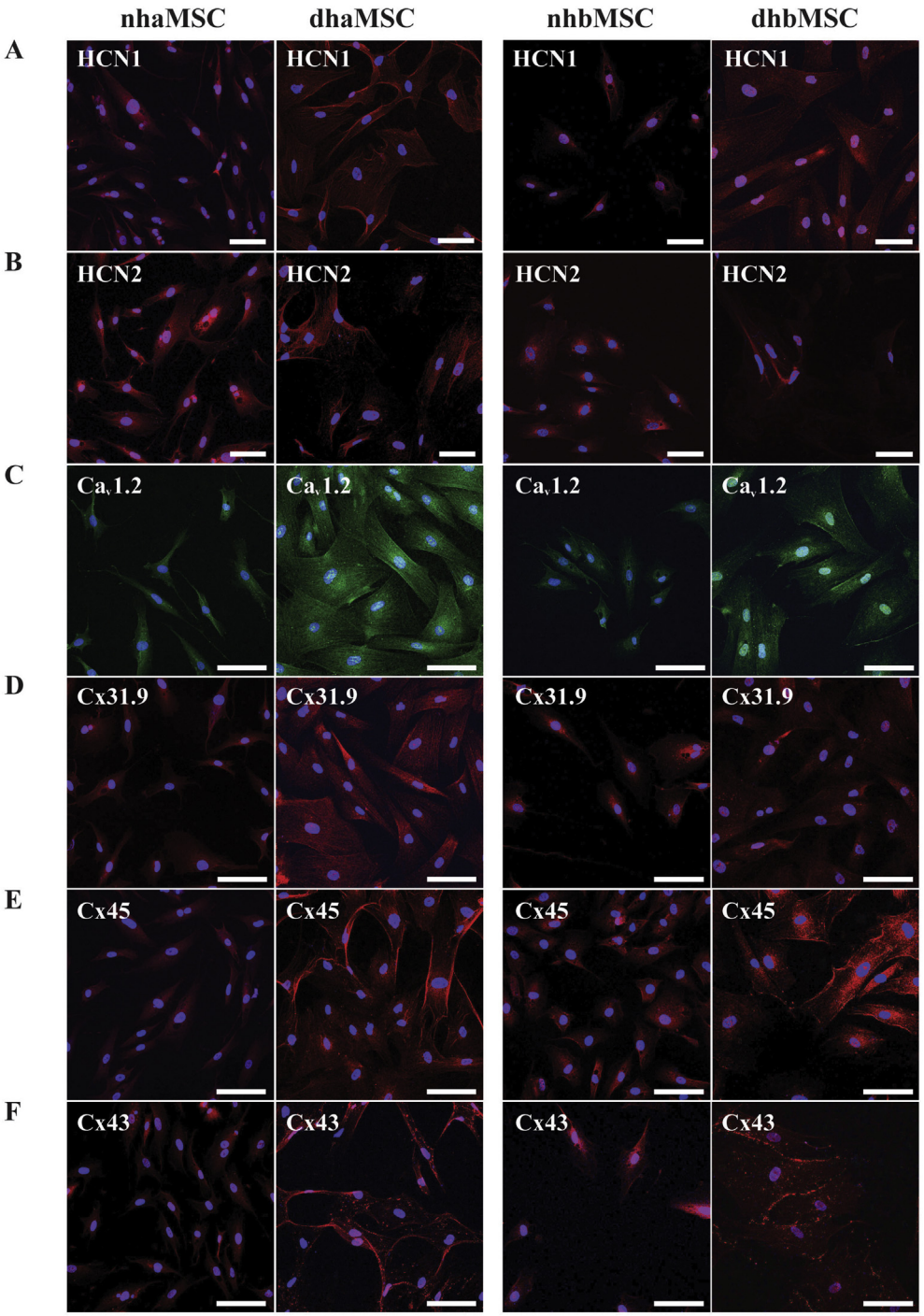

Fig. 3. Immunocytochemical analysis of haMSC (left side) and hbMSC (right side) cultured in expansion (left pannels) and differentiation medium (2 weeks, right pannels). Signals were visualized by confocal microscopy: A, anti-HCN1; B anti-HCN2; C, anti-$Ca_v1.2$; D, anti-Cx31.9; E, anti-Cx45 and F, anti-Cx43. Scale bars = 200 µm.

upon differentiation (Fig. 2, E, F), whereas transcript levels of *$Ca_v3.1$* reached levels similar to the hRA and hSAN [1] in both, dhaMSC and dhbMSC (Fig. 2, G). The alpha-subunit of the main depolarizing cardiac sodium channel *SCN5A* shows only low levels in the hSAN [1]. Likewise, transcription was found negligible in haMSC and hbMSC and remained low after differentiation in both cell types (Fig. 2, H). Inward rectifier subunit *$K_ir2.1$* was transcribed equally in both hMSC and the hSAN, with relatively high heterogeneity among different donor lineages (Fig. 2, I). Human ERG (*hERG*) transcription was very low in native haMSC and hbMSC, and showed little increase upon differentiation resulting in minor levels compared to the hRA (Fig. 2, J). *$K_v4.3$* subunits encoding for the cardiac I_{to} were transcribed low in haMSC and even lower in hbMSC (Fig. 2, K). Upon differentiation, transcription increased in both dhaMSC (5.4-fold increase, $p < 0.01$) and dhbMSC (40.3-fold increase, $p < 0.01$) (Fig. 2, K) to levels similar to those published for the hSAN [1].

3.1.4. Connexins

Gap junction proteins connect the cytoplasm of adjacent cells and are key determinants of cardiac conduction. Cx45 is specific to the hSAN and the conduction system [1,34]. Despite of low expression of Cx31.9 in the human heart, its orthologous protein Cx30.2 is

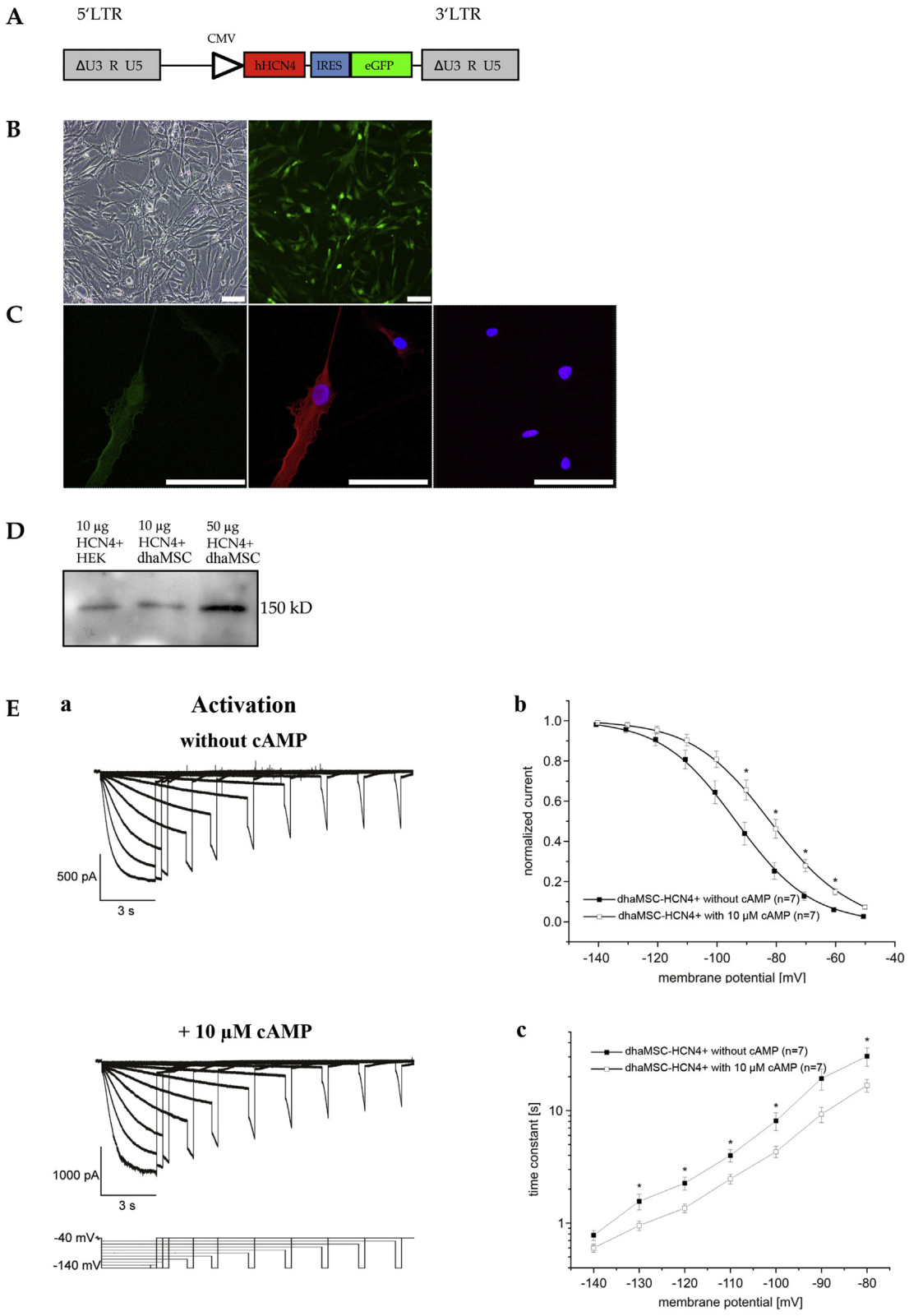

Fig. 4. Lentiviral transduction to stably transduce stem cells with the human *HCN4*-cDNA.
A, *HCN4-eGFP* vector cassette implement in lentivirus. B, light (left panel) and fluorescence (right panel) microscopy showing *HCN4-eGFP* positive dhaMSC after lentiviral transduction (MOI = 5), fluorescence activated cell sorting (FACS) and differentiation. Scale bars = 100 µm. C, Fluorescence microscopy of *HCN4-eGFP*-transduced dhaMSC. Left pannel shows eGFP signal (green), middle pannels displays anti-HCN4 positive signal (red) of the same cell. Right pannels shows non-transduced cells that are negative for anti-HCN4. Nuclei are blue, resulting from DAPI staining. Scale bars = 100 µm. D, Western blotting demonstrates *HCN4* gene transfer. Different amounts of protein from cell lysates provided evidence for HCN4 after lentiviral transduction of HEK cells (left) and dhaMSC (middle and right). E, Patch clamp electrophysiology of sorted cells provided evidence of currents with I_f characteristics showing typical cAMP responsive activation properties. Data are provided as mean ± SEM. Comparison between cAMP-stimulated ($n = 7$) and control cells (n = 7) was performed by a Student's *t*-test. Significance level: * $p < 0.05$. (For interpretation of the references to colour in this figure legend, the reader is referred to the web version of this article.)

importantly implicated in impulse delay of the cardiac conduction system in the mouse heart [35]. Cx40 and Cx43 subunits, by contrast, represent gap junctional components of the working myocardium [1,36]. Connexin transcription in hMSC was characterized by abundance of *Cx43* and low levels of *Cx40*, whereas *Cx31.9* and *Cx45* were transcribed moderately, but below published hSAN levels [1]. Differentiation resulted in a marked increase of connexin transcription, in haMSC donor line 1, in particular, leading to levels significantly higher than those published for the hSAN [1] (Fig. 2, L-O).

3.1.5. Receptors mediating response to the autonomic nervous system

As targets of neurohumoral regulation, pacemaker cells, in particular, require adrenergic (AR) and cholinergic receptors. Transcription of AR was low in native hMSC. Upon differentiation, transcription of the AR α_{1a} markedly increased in dhaMSC (124.7-fold increase compared to native haMSC, $p < 0.001$) to levels almost 10-fold higher than reference hSAN levels [1], but remained unchanged in dhbMSC (Fig. 2, P). A much lower rise upon differentiation was observed with respect to the AR β_1 in dhaMSC and dhbMSC (Fig. 2, Q). Transcription levels of the AR β_2 were strikingly increased by differentiation (4.9-fold increase in dhaMSC, $p < 0.05$, 15.5-fold increase in dhbMSC, $p < 0.01$). The cholinergic receptor *CHRM2* was absent from native hMSC but markedly upregulated in all dhaMSC donors ($p < 0.001$) (Fig. 2, S). In contrast, hbMSC showed upregualtion of *CHRM2* in dhbMSC donor 3, only (Fig. 2, S).

3.2. Comparison of transcriptional profiles

Results from transcriptional profiles and similarity to previously reported hSAN-levels [1] are summarized in Table 1. The data indicate that native haMSC produce higher levels of pacemaker gene transcripts than native hbMSC. Differentiation according to our approach resulted in a rise of pacemaker-relevant gene transcripts in both types of MSC, with transcript levels of differentiated haMSC exceeding those of differentiated hbMSC (Transcription of genes related to cardiac pacemaking in dhaMSC (mean): 8.3 ± 2.1/14 versus dhbMSC (mean): 4.3 ± 1.5/14; $p = 0.01$).

3.3. Analysis of protein distribution using immunocytochemistry

Comparative immunocytochemical analysis of important markers associated with pacemaker and cardiac function was performed in native and differentiated haMSC (line 3) and hbMSC (line 1). Immunostaining using anti-HCN1 and anti-HCN2 antibody displayed little signals in native haMSC /hbMSC membranes that increased to moderate levels upon differentiation showing higher intensity in haMSC than in hbMSC membranes (Fig. 3, A, B). In agreement with the qRT-PCR data that did not reveal *HCN4* transcripts in hMSC (Fig. 2, C), HCN4 protein could not be detected by immunocytochemistry, neither in undifferentiated nor in differentiated haMSC or hbMSC (data not shown). Consistent with the transcriptional data, providing evidence for $Ca_v1.2$ transcripts in haMSC/hbMSC, immunostaining demonstrated membrane localization of channel subunits with signals markedly increased by cell differentiation (Fig. 3, C). Immunostaining using anti-Cx31.9 antibody revealed signals at the cytoplasmic membranes with little intensity in the undifferentiated state and marked rise of signal intensity upon differentiation, higher in haMSC than in hbMSC (Fig. 3, D). Likewise, differentiation increased membrane signals for Cx45 and Cx43 in both lineages (Fig. 3, E, F).

3.4. Lentiviral HCN4-transduction leads to I_f expression in haMSC

In agreement with the absence of HCN4 in native or differentiated hMSC patch-clamp electrophysiology did not detect relevant I_f (data not shown). Because results derived from qRT-PCR and immunocytochemistry suggested differentiated haMSC more related to pacemaker cells compared to hbMSC, we used haMSC donor line 3, representative for haMSC, for transduction with an ad hoc tailored *HCN4*-lentivirus to establish long-term expression of I_f (Fig. 4, A). In vitro experiments revealed that the *HCN4-eGFP*-construct was abundantly expressed (Fig. 4, B-D) and patch clamp recordings confirmed the typical characteristics of a cAMP responsive I_f in *HCN4-eGFP* transduced dhaMSC (Fig. 4, E).

3.5. Transcription profiling of native and differentiated HCN4-transduced haMSC

We next asked whether lentiviral *HCN4*-transduction influences the transcription of genes related to pacemaking and cardiac function. When directly compared with differentiated, non-transduced haMSC cells (donor 3), dhaMSC-$HCN4^+$ showed significantly increased transcript levels of *HCN1* (2.2-fold increase, $p < 0.05$), *HCN2* (3.3-fold increase, $p < 0.05$), *Cx45* (7.7-fold increase, $p < 0.05$), *TBX3* (1.3-fold increase, $p < 0.05$), *TBX18* (1.2-fold increase, $p < 0.05$) and *SHOX2* (3.9-fold increase, $p < 0.05$). This indicates that beyond abundant *HCN4*-transcription, *HCN4* gene transfer additionally changed the transcriptional profile of important, pacemaker-relevant genes in haMSC. Moreover, adrenergic receptors important for chronotropic response were also significantly upregulated (12.2-fold increase for β_1-AR, $p < 0.05$ and 3.6-fold increase for β_2-AR, $p < 0.05$) (Fig. 5). Of note, β_1-AR was even upregulated in native haMSC-$HCN4^+$, reaching transcript levels similar to the hSAN [1] (Fig. 5, Table 1). According to this notion, the similarity of *HCN4*-transduced haMSC to the transcriptional profile of the hSAN [1] was higher than that of non *HCN4*-transduced haMSC or the non-HCN4-lentivirus transductional control and was further increased by differentiation (Table 1). However, other cardiac genes like Cx43 (1.8-fold increase, $p < 0.05$), $K_{ir}2.1$ (16.1-fold increase, $p < 0.05$) and MEF2C (8.6-fold increase, $p < 0.05$) (Fig. 5) were increased, as well, indicating that not all transcriptional changes caused by *HCN4*-transduction were towards a more nodal phenotype.

3.6. Functional characterization in a co-culture model with neonatal rat ventricular myocytes

The potential of haMSC to elicit pacemaker function was studied in a co-culture model with neonatal rat ventricular myocytes (NRVM). In an effort to address potential benefit of differentiation and/or *HCN4*-transduction, we tested native versus differentiated haMSC cultures that were either *HCN4*-transduced or untreated, using cells derived from donor 3, which showed the most representative molecular properties of the haMSC lineages tested. Parameters that were evaluated comprised earliest onset of spontaneous beating, beating rate, regularity and synchrony. NRVM monolayer characteristics were employed as baseline (Fig. 6).

3.6.1. Beating rate

Beating rate was determined daily in different co-cultures ($n = 10$ each) and in NRVM monocultures ($n = 10$) over a period of 10 days (Fig. 6, A). Co-cultures with *HCN4*-transduced haMSC displayed highest beating rates and showed longest period of spontaneous contraction (Fig. 6, A). Irrespective of *HCN4*-transduction, differentiation resulted in higher beating rates and earlier onset of spontaneous contraction. *HCN4*-transduced differentiated haMSC co-cultures showed the most favorable properties of all cultures, and were characterized by highest rates, beating onset at day 0 and longest duration of spontaneous contractions (Fig. 6, A). In contrast, co-cultures with non-*HCN4*-transduced, native haMSC showed no significant differences compared to NRVM monocultures concerning rate and duration of spontaneous beating (Fig. 6, A).

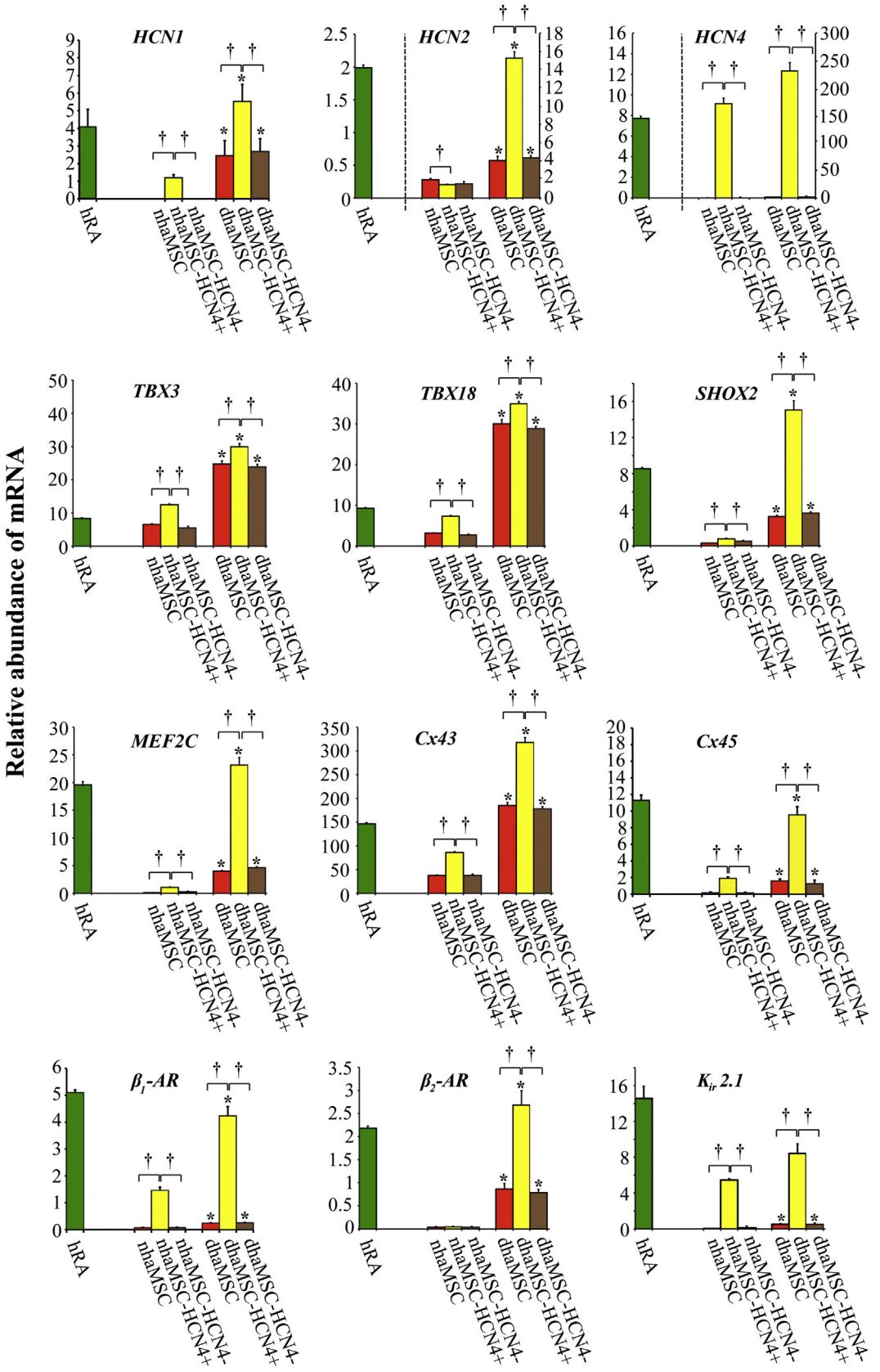

(caption on next page)

Fig. 5. Transcription profiling of genes upregulated by *HCN4*-transduction.
hRA = human right atrium (dark green); nhaMSC / dhaMSC = native / differentiated human mesenchymal stem cells from adipose tissue, donor 3 (red); nhaMSC-HCN4$^+$ / dhaMSC-HCN4$^+$ = native / differentiated human mesenchymal stem cells from adipose tissue, donor 3 with *HCN4*-transduction (yellow); nhaMSC-HCN4$^-$ / dhaMSC-HCN4$^-$ = native / differentiated human mesenchymal stem cells from adipose tissue, donor 3 with lentiviral transduction without *HCN4* (brown). * indicates the statistically significant difference between gene expression in hRA (dark green) and those in the other samples (nhaMSC, donor 3, nhaMSC-HCN4$^+$, donor 3, dhaMSC, donor 3, dhaMSC-HCN4$^+$, donor 3). The statistically significant difference between gene expression in nhaMSC / dhaMSC and that in nhaMSC-HCN4$^+$ / dhaMSC-HCN4$^+$ is indicated by an †. Data are provided as mean ± SEM. */†. $p < 0.05$. Comparison between multiple groups was performed using one-way ANOVA followed by a Tukey posthoc test. (For interpretation of the references to colour in this figure legend, the reader is referred to the web version of this article.)

3.6.2. Responsiveness to isoproterenol stimulation

We next addressed pharmacological responsiveness upon simulation with isoproterenol on co-culture day 4 (Fig. 6, B). Dishes containing *HCN4*-transduced haMSC showed significantly higher responsiveness towards isoproterenol stimulation than non-transduced haMSC or NRVM monolayer (Fig. 6, B). Although total beating rate was highest in co-culture dishes with differentiated *HCN4*-transduced haMSC, rate increase was not significantly different from native *HCN4*-transduced haMSC, indicating that membrane presence of *HCN4*-channels but not differentiation mainly determine increased responsiveness to isoproterenol (Fig. 6, B).

3.6.3. Stability of beating rate

Dishes containing differentiated *HCN4*-transduced haMSC showed highest stability of physiological beating rates throughout the observational period (day 1 to 7, mean rate 84 ± 7.1 bpm, Table 2), whereas *HCN4*-transduced non-differentiated dishes showed highest rate of 140 bpm at day 3, declining rapidly thereafter, characteristic for a higher rate variance (mean rate 71 ± 9.4 bpm, Table 2). Dishes containing haMSC either differentiated or not, displayed relatively high dispersion of rate.

3.6.4. Regularity and synchrony

We evaluated intracellular regularity by measuring calcium-transients in cardiac myocytes at day 4 of co-cultures. Calcium-transients were strikingly more regular in dishes that contained differentiated haMSC (Fig. 6, C), as evaluated by Poincaré plots (Fig. 7) and SD1/SD2 analysis (Fig. 7F, G). Interestingly, this effect was independent of *HCN4* gene transfer as regularity of co-cultures containing *HCN4*-transduced but non-differentiated haMSC remained low, while beating rate was markedly increased by *HCN4*-transduction (Fig. 7F, G). Thus, co-cultures with differentiated *HCN4*-transduced haMSC displayed highest beating rate (Fig. 6, C) and regularity (Fig. 7).

We next asked whether beating was synchronous within the culture dish, or characterized by foci of cardiac myocytes that were beating independently from each other. Foci in baseline NRVM monolayer dishes showed high asynchrony and were easily to distinguish by their different beating characteristics (Fig. 6, C, upper and lower diagram of calcium transients in NRVM monocultures not superposable). Addition of undifferentiated haMSC did not significantly change this pattern (Fig. 6, C, upper and lower diagram of calcium transients in undifferentiated haMSC with and without *HCN4*-transduction not superposable). Addition of differentiated haMSC, in contrast, significantly increased synchrony and beating characteristics of foci appeared more confluent (Fig. 6, C, upper and lower diagram of calcium transients in differentiated haMSC nearly superposable). Addition of differentiated *HCN4*-transduced haMSC induced a highly synchronous beating pattern (Fig. 6, C, upper and lower diagram of calcium transients in differentiated *HCN4*-transduced haMSC completely superposable). Thus, co-cultures with differentiated haMSC displayed more pronounced regularity and synchrony of beating rate (Video S1) than co-cultures with undifferentiated haMSC or NRVM-monocultures (Video S2).

3.7. Cell-cell contacts between differentiated haMSC and NRVM

Given the high regularity and synchrony in co-cultures with differentiated haMSC (Fig. 7), we next asked for connexins expression in the co-culture. To this end, we performed immunohistochemistry of co-cultures of *HCN4*- (*eGFP*) -transduced dhaMSC with NRVM, using anti-Cx43 antibody (Fig. 3E). Confocal imaging revealed co-localization of differentiated haMSC with NRVM pointing to Cx43 positive cell-cell contacts (Fig. 8), which may underlie electrical coupling between both cell types.

4. Discussion

Cell-based therapy is a promising approach for cardiac tissue regeneration and repair. MSC are attractive candidates as they are easily obtained from bone marrow aspirates or adipose tissue, can be expanded to high numbers in vitro and show the ability to differentiate into several mesenchymal cell lineages, including cells with myogenic characteristics [37]. Applied in an allogeneic setting, MSC were reported not to induce immune responses or inflammation [38–40]. However, the efficacy of MSC differentiation into cardiomyocyte is limited as transdifferentiation requires potentially teratogenic substances like 5-azacytidine (5-aza) or amphotericin (AMPH), hampering its use with respect to a future clinical application [41,42]. Furthermore, aiming at the development of an electrically active cell system, native MSC lack depolarizing current [43] and might not adequately electrically integrate within myocardial syncytium [44,45]. Genetically modified MSC expressing the pacemaker current I_f were reported to produce rhythmic depolarizing potentials and conduct theses potential to adjacent cardiomyocytes by gap junctional coupling, according to a „two-cell functional syncytium “[46]. Based on this notion, pacemaker potential generated in MSC may employ sodium current of the adjacent myocyte to elicit action potentials [46]. Thus, connexin-mediated electrical intercellular connections are key factors for MSC-based biological pacemaker systems. In this regard, cell-cell interaction of MSC to adjacent myocytes were shown to primarily consist of connexins 43, abundantly expressed by MSC but not a pacemaker-specific connexin.

In the present study we addressed the capability of human mesenchymal stem cells (hMSC) derived from adipose tissue or bone marrow, to acquire “nodal-like” properties by modification of culture conditions. Initially, several differentiation protocols, excluding teratogenic or oncogenic substances, were tested and expression of pacemaker hallmark genes was studied. We developed a differentiation protocol effective to upregulate several important genes relevant to cardiac pacemaking in hMSC. This medium comprises RPMI-B27, initially developed for the serum-free growth of hippocampal neurons [47], but also was proven effective for the cardiomyogenic differentiation of human embryonic stem cells [18]. RPMI-B27 was further supplemented with BMP4 resulting in improved pacemaker-type gene expression. Culturing of hMSC for 2 weeks according to our approach gave rise to abundant expression of connexins 31.9, 43 and 45, depolarizing $Ca_v1.2$, $Ca_v1.3$, HCN1 and 2 channel subtypes, adrenergic receptors α_{1a} and β_2 and the muscarinic acetylcholine receptor-2 gene (CHRM2). Of note, adipose-derived hMSC (haMSC) exhibited properties more favorable with respect to pacemaker cell characteristics than bone-marrow derived hMSC (hbMSC). In fact, SAN-typical transcription factors TBX3, 18, and SHOX2 [48–50] were significantly upregulated upon differentiation. Furthermore, our data reveal that addition of BMP4 to the medium leads to significant upregulation of SHOX2 and

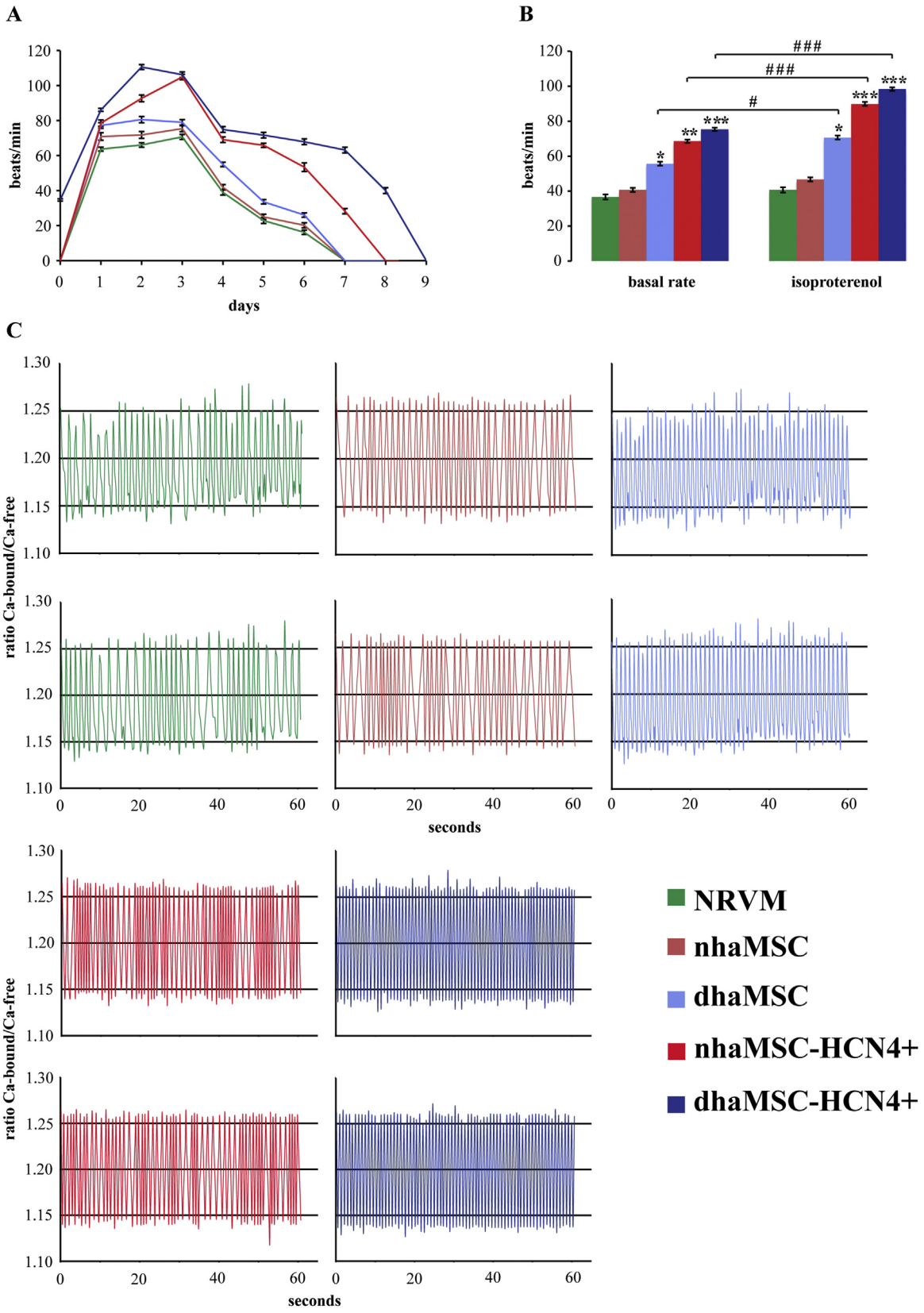

Fig. 6. Functional characterization of modified haMSC in co-culture with neonatal rat ventricular myocytes (NRVM).
A, Spontaneous beating frequency of NRVM monoculture (green) and co-cultures NRVM + nhaMSC (pink), NRVM + dhaMSC (light blue), NRVM + nhaMSC-HCN4$^+$ (red), and NRVM + dhaMSC-HCN4$^+$ (dark blue) over time. B, Stimulation of NRVM monoculture and co-cultures with 1 μM isoproterenol. C, Measurement of calcium spikes in NRVM monocultures as well as in cocultures. They were measured at two different sites of the NRVM monocultures or co-cultures. * $p < 0.05$; ** $p < 0.01$; *** $p < 0.001$. Several groups were compared by one-way ANOVA (analysis of variance), followed by a post-hoc test (Tukey's test). (For interpretation of the references to colour in this figure legend, the reader is referred to the web version of this article.)

Table 2
Beating rates of co-cultures with *HCN4*-transduced haMSC.

	Beating rate (arithmetic mean + SEM)	
	nhaMSC-HCN4 + /NRVM	dhaMSC-HCN4$^+$/NRVM
Day 1	80 ± 1.5 beats/min	88 ± 1.7 beats/min
Day 2	91 ± 2.4 beats/min	111 ± 1.9 beats/min
Day 3	105 ± 1.7 beats/min	106 ± 1.8 beats/min
Day 4	70 ± 2.1 beats/min	78 ± 2.2 beats/min
Day 5	65 ± 1.2 beats/min	73 ± 2.4 beats/min
Day 6	53 ± 2.5 beats/min	68 ± 2.3 beats/min
Day 7	30 ± 1.9 beats/min	62 ± 2.5 beats/min
Average day 1 to day 7	71 ± 9.4 beats/min	84 ± 7.1 beats/min

(consequently) BMP4, given that SHOX2 activates BMP4 implicated in early sinoatrial development [31]. This points to a potential positive feedback-loop potentiating "nodal" development in a specific intracardiac microenvironment. However, not all differentiation-induced transcriptional changes were directed towards a more nodal phenotype. Levels of Cx43, known to be highly expressed in native MSC, were even increased by differentiation. Although Cx43 is not pacemaker-typical, previous research has found that high Cx43-mediated conductance is beneficial for electrical signal transmission from cells with pacemaker characteristics to neighbor cardiomyocytes [46,51]. Moreover, HCN4 channels considered to contribute importantly to spontaneous depolarization in SAN cells were absent in both, differentiated haMSC and hbMSC. HCN1, recently proposed as a highly specific SAN marker in humans in a study directly evaluating HCN protein expression in human SAN pacemaker tissue [33], was significantly increased in differentiated haMSC in particular, but showed only moderate presence in the cell membrane. Consistently, no relevant I_f was detected in haMSC or hbMSC, limiting their capability to elicit upstroke potential. To substitute for I_f, a lentivirus was generated for stable gene transfer of human *HCN4* cDNA. Patch clamp recordings of HCN4-transduced, differentiated haMSC provided evidence of abundant current with I_f characteristics showing typical cAMP responsive activation.

To evaluate the functional effects of haMSC within cardiac environment we established an in vitro co-culture model with neonatal rat ventricular myocytes (NRVM). We compared native versus differentiated haMSC that were either *HCN4*-transduced or non-transduced and co-cultured them with NRVM. Results demonstrated that co-culturing with *HCN4*-transduced haMSC gave rise to a significantly earlier onset of spontaneous contractions and higher beating rates compared to non-transduced haMSC or baseline NRVM. Furthermore, differentiated haMSC elicited a much higher regularity and intercellular beating synchrony when co-cultured with NRVM. In contrast, non-differentiated haMSC containing dishes and baseline NRVM monolayers were characterized by irregular beating and multiple centers of activity, lacking synchronous contraction. This suggests that more HCN4 current may be transferred from differentiated haMSC-HCN4$^+$ to adjacent NRVMs than in the undifferentiated state, most likely due to an increased connexins-mediated conduction, leading to high regularity and synchrony. In line with that, lentiviral *HCN4* gene transfer of NRVMs has previously been reported to increase and stabilize beating rate after a critical level of gene transfer was reached [52].

We next addressed pharmacological responsiveness of co-cultures. *HCN4*-transduced haMSC exerted marked influence on beating rate of co-cultures in response to adrenergic stimulation. Upon addition of isoproterenol, haMSC-HCN4$^+$ containing dishes showed highest rate response (51 ± 9% faster than at baseline) compared to non-transduced co-cultures or NRVM monolayer. These results are in line with qRT-PCR data providing evidence for adrenergic receptor transcripts highest in differentiated haMSC, pointing to intact second messenger mediated intracellular activation of I_f.

Thus, the combination of RPMI-B27 + BMP4 mediated differentiation together with *HCN4*-transduction of haMSC produced a cell type that initiated earliest beating onset and highest rates, synchronization, regularity and rate responsiveness of co-cultures. However, despite the induction of important nodal transcription factors (e.g. Tbx3, Tbx18, Shox2) by differentiation, dhaMSC still showed abundant "non-nodal" Cx43 expression and lacked HCN4, indicating a limited potential of MSC to achieve properties identical to a unique SAN cell. Cell-coupling of cardiomyocytes to the SAN and the conduction system is uniquely characterized by structures that facilitate impulse delay, in particular Cx45 in the human SAN and Cx30.2 (orthologous of human Cx31.9) in the mouse conduction system to protect from fast rate and overdrive pacing [35]. A benefit of viral co-transduction of MSC with *HCN4* and *Cx45* to establish biological pacemaking was recently reported [53]. As shown here, high expression of connexins can be achieved by modification of culture media to waive the requirement of additional lentiviral gene transfer. Thus, from a translational point of view differentiated haMSC may constitute a cell source with significantly improved properties for pacemaker current delivery to the myocardium. However, it remains to be addressed by future studies, whether abundant but somehow unspecific expression of connexins by differentiated haMSC may facilitate proper and sustained biological pacemaking in vivo.

5. Limitations

The experimental co-culture in vitro system to model cellular pacemaker function comprises important limitations in the assessment of factors crucial for biological pacemaking such as functional and anatomical in situ integration, immunotolerance, and persistence of spontaneous activity. Furthermore, differentiation potential of MSC to achieve cardiomyogenic properties in general and nodal-type characteristics in particular, is limited compared to cells with higher plasticity (e.g. embryonic or induced pluripotent stem cells). However, native MSC expressing pacemaker channels by viral gene transfer were successfully utilized as biological pacemakers in previous large animal studies [13,14] but pacing rate and persistence of cell therapies remained shortcomings, raising the question whether and how in vitro pre-conditioning of MSC might lead to a more nodal-type commitment of cells. Here we have investigated the utility of differentiated haMSC and hbMSC in combination with lentiviral gene transfer of HCN4 to achieve cells with pacemaker characteristics. It remains of interest whether substitution for HCN1, recently identified as even more specific in the human SAN [33] than HCN4, may elicit a superior nodal-type cellular profile in MSC with respect to a unique human SAN cell.

6. Conclusions

Our data reveal that human adipose tissue derived haMSC can be partly differentiated towards a nodal phenotype, rather than bone marrow derived hbMSC, using a specified culture medium (RPMI-B27 + BMP4 supplement). However, "nodal-type" expression could not be reproduced completely, lacking adequate levels of HCN channels and cardiac structure proteins, while connexin levels increased but remained rather unspecific. Introduction of HCN4 by lentiviral gene transfer resulted in an improved pacemaker-type transcription profile, earlier onset of spontaneous contractions, and higher beating synchrony and rate in co-culture experiments of differentiated haMSC-HCN4$^+$ with NRVM. Notably, differentiation and substitution for HCN4 markedly increased connexin levels, which in consequence significantly improved regularity of co-cultures, indicating a better connexin-mediated transmission of depolarizing current from differentiated haMSC-HCN4$^+$ to adjacent cardiomyocytes.

Supplementary data to this article can be found online at https://doi.org/10.1016/j.lfs.2019.116620.

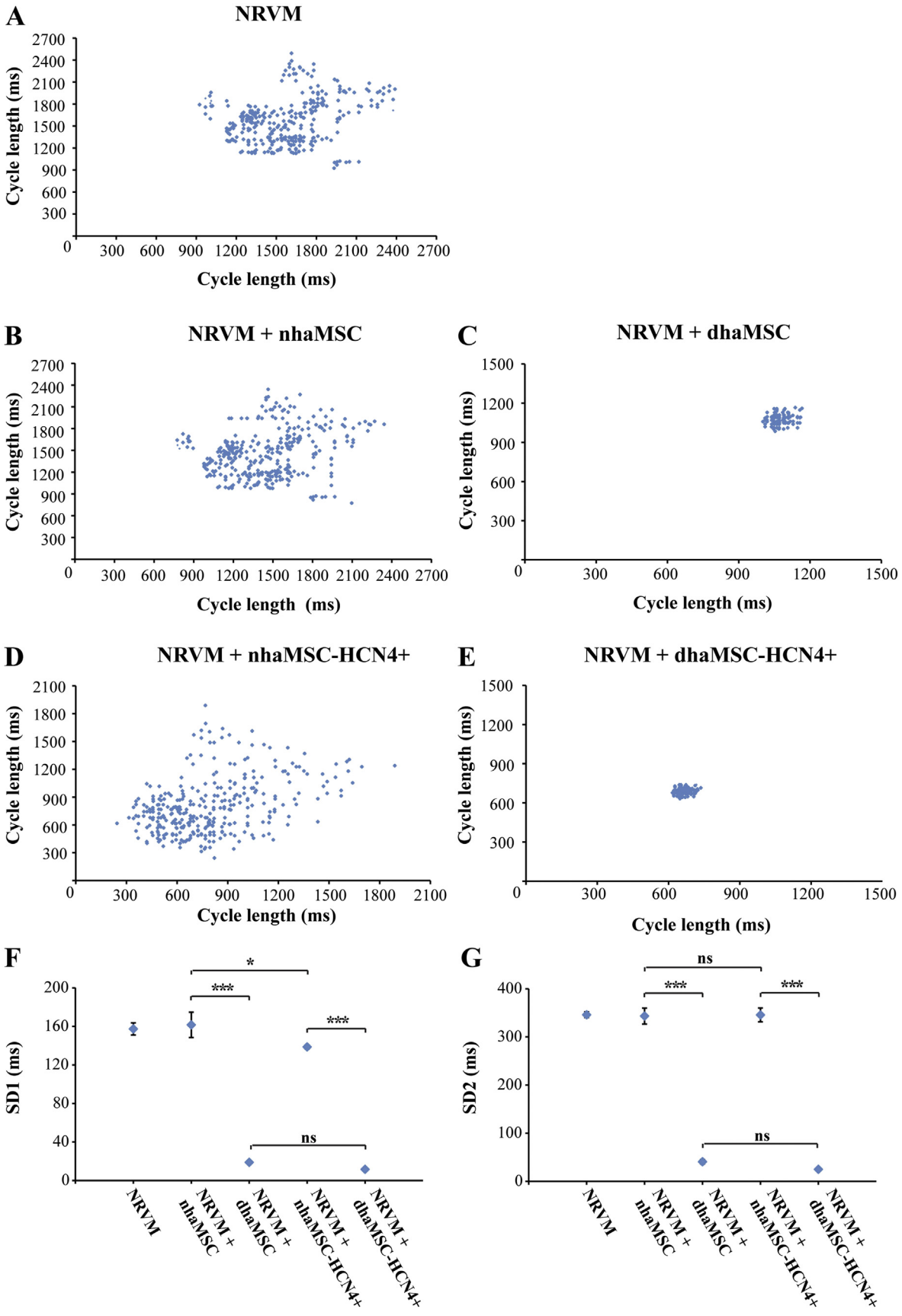

(caption on next page)

Fig. 7. Illustration of beating rate regularity by Poincaré plots.
A, B, D, Poincaré plots of NRVM monocultures and of co-cultures with native haMSC or native haMSC-HCN4$^+$ displayed a high beat-to-beat dispersion, thus illustrating the irregular beating pattern of these cultures. C, E, Poincaré plots of co-cultures with differentiated haMSC or differentiated haMSC-HCN4$^+$ showed, by contrast, a very low beat-to-beat dispersion, hence visualizing the high regularity of beating rate in these cultures. F, G, standard deviation 1 (SD1) and standard deviation 2 (SD2) of NRVM monocultures and co-cultures with native haMSC or native haMSC-HCN4$^+$ are significantly higher than in co-cultures with differentiated haMSC or differentiated haMSC-HCN4$^+$ ($p < 0.001$). SD1 and SD2 are provided as mean ± SD. * $p < 0.05$, *** $p < 0.001$ ($n = 3$). Comparison between multiple groups was performed using one-way ANOVA followed by a Tukey posthoc test.

Fig. 8. Confocal imaging of co-culture indicates cell-cell contacts between differentiated haMSC-HCN4$^+$ and adjacent NRVM. Note Cx43 signals (red) of NRVM but also detectable at membranes of adjacent differentiated haMSC-HCN4$^+$ suggesting connexin-mediated coupling of cells. Nuclei are blue, resulting from DAPI staining. Scale bars = 100 µm. (For interpretation of the references to colour in this figure legend, the reader is referred to the web version of this article.)

Author contributions

Conceptualization, Fabrice F. Darche and Patrick A. Schweizer; Methodology, Fabrice F. Darche and Patrick A. Schweizer; Software, Fabrice F. Darche; Validation, Fabrice F. Darche and Patrick A. Schweizer; Formal Analysis, Fabrice F. Darche and Patrick A. Schweizer; Investigation, Fabrice F. Darche and Patrick A. Schweizer; Resources, Fabrice F. Darche, Eva Köllensperger, Uwe Leimer, Günter Germann, Anja Seckinger, Dirk Hose and Patrick A. Schweizer; Data Curation, Fabrice F. Darche and Patrick A. Schweizer; Roles/Writing – Original Draft, Fabrice F. Darche and Patrick A. Schweizer; Writing – Review & Editing, Fabrice F. Darche, Rasmus Rivinius, Eva Köllensperger, Uwe Leimer, Günter Germann, Anja Seckinger, Dirk Hose, Julian Schröter, Claus Bruehl, Andreas Draguhn, Richard Gabriel, Manfred Schmidt, Michael Koenen, Dierk Thomas, Hugo A. Katus and Patrick A. Schweizer; Visualization, Fabrice F. Darche and Patrick A. Schweizer; Supervision, Michael Koenen, Dierk Thomas, Hugo A. Katus and Patrick A. Schweizer; Project Administration, Patrick A. Schweizer; Funding Acquisition, Fabrice F. Darche, Dierk Thomas, Hugo A. Katus and Patrick A. Schweizer.

Funding

This research was funded in parts by grants from the Deutsche Forschungsgemeinschaft (SCHW 1611/1-1 to Patrick A. Schweizer and TH 1120/8-1 to Dierk Thomas), from the Max-Planck-Society (TANDEM project to Patrick A. Schweizer), from the German Cardiac Society and the Hengstberger Foundation (Klaus-Georg and Sigrid Hengstberger Scholarship to Dierk Thomas), from the Ministry of Science, Research and Art Baden-Württemberg (Sonderlinie Medizin to Dierk Thomas), from the German Heart Foundation (Kaltenbach scholarship to Fabrice F. Darche), from the Heidelberg Medical Faculty (*Physician Scientist-Programm* to Fabrice F. Darche) and from the German Centre for Cardiovascular Research (DZHK). Patrick A. Schweizer is recipient of the Heidelberg Research Center for Molecular Medicine (HRCMM) Senior Career Fellowship.

Declaration of Competing Interest

The authors declare that there are no conflicts of interest.

Acknowledgments

We thank Simone Bauer and Marit Hubrecht for the excellent technical work. We thank Prof. Luigi Naldini for having provided the lentiviral plasmid construct pCCLsin.cPPT.SFFV.IRES.eGFP.WPRE.

References

[1] N.J. Chandler, I.D. Greener, J.O. Tellez, S. Inada, H. Musa, P. Molenaar, D. Difrancesco, M. Baruscotti, R. Longhi, R.H. Anderson, R. Billeter, V. Sharma, D.C. Sigg, M.R. Boyett, H. Dobrzynski, Molecular architecture of the human sinus node: insights into the function of the cardiac pacemaker, Circulation 119 (2009) 1562–1575, https://doi.org/10.1161/CIRCULATIONAHA.108.804369.
[2] D. DiFrancesco, P. Tortora, Direct activation of cardiac pacemaker channels by intracellular cyclic AMP, Nature 351 (1991) 145–147, https://doi.org/10.1038/351145a0.
[3] D. DiFrancesco, The hyperpolarization-activated (If) current: Autonomic regulation and the control of pacing, in: M. Morad, S. Ebashi, W. Trautwein, Y. Kurachi (Eds.), Molecular Physiology and Pharmacology of Cardiac Ion Channels and Transporters, Kluwer Academic Publishers, Dordrecht, The Netherlands, 1996, pp. 31–37.
[4] A. Bucchi, M. Baruscotti, R.B. Robinson, D. DiFrancesco, Modulation of rate by autonomic agonists in SAN cells involves changes in diastolic depolarization and the pacemaker current, J. Mol. Cell. Cardiol. 43 (2007) 39–48, https://doi.org/10.1016/j.yjmcc.2007.04.017.
[5] P.A. Schweizer, N. Duhme, D. Thomas, R. Becker, J. Zehelein, A. Draguhn, C. Bruehl, H.A. Katus, M. Koenen, cAMP sensitivity of HCN pacemaker channels determines basal heart rate but is not critical for autonomic rate control, Circ. Arrhythm. Electrophysiol. 1 (2010) 542–552, https://doi.org/10.1161/CIRCEP.110.949768.
[6] N. Duhme, P.A. Schweizer, D. Thomas, R. Becker, J. Schröter, T.R. Barends, I. Schlichting, A. Draguhn, C. Bruehl, H.A. Katus, M. Koenen, Altered HCN4 channel C-linker interaction is associated with familial tachycardia-bradycardia syndrome and atrial fibrillation, Eur. Heart J. 34 (2013) 2768–2775, https://doi.org/10.1093/eurheartj/ehs391.
[7] P.A. Schweizer, J. Schröter, S. Greiner, J. Haas, P. Yampolsky, D. Mereles, S.J. Buss, C. Seyler, C. Bruehl, A. Draguhn, M. Koenen, B. Meder, H.A. Katus, D. Thomas, The symptom complex of familial sinus node dysfunction and myocardial noncompaction is associated with mutations in the HCN4 channel, J. Am. Coll. Cardiol. 64 (2014) 757–767, https://doi.org/10.1016/j.jacc.2014.06.1155.
[8] M.R. Rosen, R.B. Robinson, P.R. Brink, I.S. Cohen, The road to biological pacing, Nat. Rev. Cardiol. 8 (2011) 656–666, https://doi.org/10.1038/nrcardio.2011.120.
[9] M.R. Rosen, Gene therapy and biological pacing, N. Engl. J. Med. 371 (2014) 1158–1159, https://doi.org/10.1056/NEJMcibr1408897.
[10] E. Cingolani, J.I. Goldhaber, E. Marbán, Next-generation pacemakers: from small devices to biological pacemakers, Nat. Rev. Cardiol. 15 (2018) 139–150, https://doi.org/10.1038/nrcardio.2017.165.
[11] P.A. Schweizer, F.F. Darche, N.D. Ullrich, P. Geschwill, B. Greber, R. Rivinius, C. Seyler, K. Müller-Decker, A. Draguhn, J. Utikal, M. Koenen, H.A. Katus, D. Thomas, Subtype-specific differentiation of cardiac pacemaker cell clusters from human induced pluripotent stem cells, Stem Cell Res Ther 8 (2017) 229, , https://doi.org/10.1186/s13287-017-0681-4.
[12] H.C. Cho, E. Marbán, Biological therapies for cardiac arrhythmias: can genes and cells replace drugs and devices? Circ. Res. 106 (2010) 674–685, https://doi.org/10.1161/CIRCRESAHA.109.212936.

[13] A.N. Plotnikov, I. Shlapakova, M.J. Szabolcs, P. Danilo Jr., B.H. Lorell, I.A. Potapova, Z. Lu, A.B. Rosen, R.T. Mathias, P.R. Brink, R.B. Robinson, I.S. Cohen, M.R. Rosen, Xenografted adult human mesenchymal stem cells provide a platform for sustained biological pacemaker function in canine heart, Circulation 116 (2007) 706–713, https://doi.org/10.1161/CIRCULATIONAHA.107.703231.

[14] W. Lu, N. Yaoming, R. Boli, C. Jun, Z. Changhai, Z. Yang, S. Zhiyuan, mHCN4 genetically modified canine mesenchymal stem cells provide biological pacemaking function in complete dogs with atrioventricular block, Pacing Clin. Electrophysiol. 36 (2013) 1138–1149, https://doi.org/10.1111/pace.12154.

[15] M. Reyes, C.M. Verfaillie, Characterization of multipotent adult progenitor cells, a subpopulation of mesenchymal stem cells, Ann. N. Y. Acad. Sci. 938 (2001) 231–233.

[16] E. Koellensperger, W. Niesen, J. Kolbenschlag, F. Gramley, G. Germann, U. Leimer, Human adipose tissue derived stem cells promote liver regeneration in a rat model of toxic injury, Stem Cells Int. (2013) 534263, , https://doi.org/10.1155/2013/534263.

[17] J.L. Spees, S.D. Olson, J. Ylostalo, P.J. Lynch, J. Smith, A. Perry, A. Peister, M.Y. Wang, D.J. Prockop, Differentiation, cell fusion, and nuclear fusion during ex vivo repair of epithelium by human adult stem cells from bone marrow stroma, Proc. Natl. Acad. Sci. U. S. A. 100 (2003) 2397–2402, https://doi.org/10.1073/pnas.0437997100.

[18] M.A. Laflamme, K.Y. Chen, A.V. Naumova, V. Muskheli, J.A. Fugate, S.K. Dupras, H. Reinecke, C. Xu, M. Hassanipour, S. Police, C. O'Sullivan, L. Collins, Y. Chen, E. Minami, E.A. Gill, S. Ueno, C. Yuan, J. Gold, C.E. Murry, Cardiomyocytes derived from human embryonic stem cells in pro-survival factors enhance function of infarcted rat hearts, Nat. Biotechnol. 25 (2007) 1015–1024, https://doi.org/10.1038/nbt1327.

[19] T. Dull, R. Zufferey, M. Kelly, R.J. Mandel, M. Nguyen, D. Trono, L. Naldini, A third-generation lentivirus vector with a conditional packaging system, J. Virol. 72 (1998) 8463–8471.

[20] A. Follenzi, L.E. Ailles, S. Bakovic, M. Geuna, L. Naldini, Gene transfer by lentiviral vectors is limited by nuclear translocation and rescued by HIV-1 pol sequences, Nat. Genet. 25 (2000) 217–222, https://doi.org/10.1038/76095.

[21] C. Demaison, K. Parsley, G. Brouns, M. Scherr, K. Battmer, C. Kinnon, M. Grez, A.J. Thrasher, High-level transduction and gene expression in hematopoietic repopulating cells using a human immunodeficiency [correction of imunodeficiency] virus type 1-based lentiviral vector containing an internal spleen focus forming virus promoter, Hum. Gene Ther. 13 (2002) 803–813, https://doi.org/10.1089/10430340252898984.

[22] E. Martinez-Salas, Internal ribosome entry site biology and its use in expression vectors, Curr. Opin. Biotechnol. 10 (1999) 458–464.

[23] J. Qiao, V. Roy, M.H. Girard, M. Caruso, High translation efficiency is mediated by the encephalomyocarditis virus internal ribosomal entry sites if the natural sequence surrounding the eleventh AUG is retained, Hum. Gene Ther. 13 (2002) 881–887, https://doi.org/10.1089/10430340252899046.

[24] K.J. Livak, T.D. Schmittgen, Analysis of relative gene expression data using real-time quantitative PCR and the 2(−Delta Delta C(T)) method, Methods 25 (2001) 402–408, https://doi.org/10.1006/meth.2001.1262.

[25] P.A. Schweizer, P. Yampolsky, R. Malik, D. Thomas, J. Zehelein, H.A. Katus, M. Koenen, Transcription profiling of HCN-channel isotypes throughout mouse cardiac development, Basic Res. Cardiol. 104 (2009) 621–629, https://doi.org/10.1007/s00395-009-0031-5.

[26] M.D. Harrell, S. Harbi, J.F. Hoffman, J. Zavadil, W.A. Coetzee, Large-scale analysis of ion channel gene expression in the mouse heart during perinatal development, Physiol. Genomics 28 (2007) 273–283, https://doi.org/10.1152/physiolgenomics.00163.2006.

[27] P. Most, M. Boerries, C. Eicher, C. Schweda, P. Ehlermann, S.T. Pleger, E. Loeffler, W.J. Koch, H.A. Katus, C.A. Schoenenberger, A. Remppis, Extracellular S100A1 protein inhibits apoptosis in ventricular cardiomyocytes via activation of the extracellular signal-regulated protein kinase 1/2 (ERK1/2), J. Biol. Chem. 278 (2003) 48404–48412, https://doi.org/10.1074/jbc.M308587200.

[28] M. Brennan, M. Palaniswami, P. Kamen, Do existing measures of poincare plot geometry reflect nonlinear features of heart rate variability, IEEE Trans on Biomed Engg 48 (2001) 1342–1347, https://doi.org/10.1109/10.959330.

[29] V.M. Christoffels, M.T. Mommersteeg, M.O. Trowe, O.W. Prall, C. de Gier-de Vries, A.T. Soufan, M. Bussen, K. Schuster-Gossler, R.P. Harvey, A.F. Moorman, A. Kispert, Formation of the venous pole of the heart from an Nkx2-5-negative precursor population requires Tbx18, Circ. Res. 98 (2006) 1555–1563, https://doi.org/10.1161/01.RES.0000227571.84189.65.

[30] A. Sizarov, H.D. Devalla, R.H. Anderson, R. Passier, V.M. Christoffels, A.F. Moorman, Molecular analysis of patterning of conduction tissues in the developing human heart, Circ. Arrhythm. Electrophysiol. 4 (2011) 532–542, https://doi.org/10.1161/CIRCEP.111.963421.

[31] S. Puskaric, S. Schmitteckert, A.D. Mori, A. Glaser, K.U. Schneider, B.G. Bruneau, R.J. Blaschke, H. Steinbeisser, G. Rappold, Shox2 mediates Tbx5 activity by regulating Bmp4 in the pacemaker region of the developing heart, Hum. Mol. Genet. 19 (2010) 1425–1433, https://doi.org/10.1093/hmg/ddq393.

[32] C. Marionneau, B. Couette, J. Liu, H. Li, M.E. Mangoni, J. Nargeot, M. Lei, D. Escande, S. Demolombe, Specific pattern of ionic channel gene expression associated with pacemaker activity in the mouse heart, J. Physiol. 562 (2005) 223–234, https://doi.org/10.1113/iphysiol.2004.074047.

[33] N. Li, T.A. Csepe, B.J. Hansen, H. Dobrzynski, R.S. Higgins, A. Kilic, P.J. Mohler, P.M. Janssen, M.R. Rosen, B.J. Biesiadecki, V.V. Fedorov, Molecular mapping of sinoatrial node HCN channel expression in the human heart, Circ. Arrhythm. Electrophysiol. 8 (2015) 1219–1227, https://doi.org/10.1161/CIRCEP.115.003070.

[34] J.A. Jansen, T.A. van Veen, J.M. de Bakker, H.V. van Rijen, Cardiac connexins and impulse propagation, J. Mol. Cell. Cardiol. 48 (2010) 76–82, https://doi.org/10.1016/j.yjmcc.2009.08.018.

[35] M.M. Kreuzberg, M. Liebermann, S. Segschneider, R. Dobrowolski, H. Dobrzynski, R. Kaba, G. Rowlinson, E. Dupont, N.J. Severs, K. Willecke, Human connexin31.9, unlike its orthologous protein connexin30.2 in the mouse, is not detectable in the human cardiac conduction system, J. Mol. Cell. Cardiol. 46 (2009) 553–559, https://doi.org/10.1016/j.yjmcc.2008.12.007.

[36] N. Gaborit, S. Le Bouter, V. Szuts, A. Varro, D. Escande, S. Nattel, S. Demolombe, Regional and tissue specific transcript signatures of ion channel genes in the non-diseased human heart, J. Physiol. 582 (2007) 675–693, https://doi.org/10.1113/jphysiol.2006.126714.

[37] M. Shiota, T. Heike, M. Haruyama, S. Baba, A. Tsuchiya, H. Fujino, H. Kobayashi, T. Kato, K. Umeda, M. Yoshimoto, T. Nakahata, Isolation and characterization of bone marrow-derived mesenchymal progenitor cells with myogenic and neuronal properties, Exp. Cell Res. 313 (2007) 1008–1023, https://doi.org/10.1016/j.yexcr.2006.12.017.

[38] M.F. Pittenger, B.J. Martin, Mesenchymal stem cells and their potential as cardiac therapeutics, Circ. Res. 95 (2004) 9–20, https://doi.org/10.1161/01.RES.0000135902.99383.6f.

[39] P.A. Schweizer, U. Krause, R. Becker, A. Seckinger, A. Bauer, C. Hardt, V. Eckstein, A.D. Ho, M. Koenen, H.A. Katus, J. Zehelein, Atrial-radiofrequency catheter ablation mediated targeting of mesenchymal stem cells, Stem Cells 25 (2007) 1546–1551, https://doi.org/10.1634/stemcells.2006-0682.

[40] P. Niemeyer, M. Kornacker, A. Mehlhorn, A. Seckinger, J. Vohrer, H. Schmal, P. Kasten, V. Eckstein, N.P. Südkamp, U. Krause, Comparison of immunological properties of bone marrow stromal cells and adipose tissue-derived stem cells before and after osteogenic differentiation in vitro, Tissue Eng. 13 (2007) 111–121, https://doi.org/10.1089/ten.2006.0114.

[41] N.S. Ye, J. Chen, G.A. Luo, R.L. Zhang, Y.F. Zhao, Y.M. Wang, Proteomic profiling of rat bone marrow mesenchymal stem cells induced by 5-azacytidine, Stem Cells Dev. 15 (2006) 665–676, https://doi.org/10.1089/scd.2006.15.665.

[42] G. Yang, J. Tian, C. Feng, L.L. Zhao, Z. Liu, J. Zhu, Trichostatin A promotes cardiomyocyte differentiation of rat mesenchymal stem cells after 5-azacytidine induction or during co-culture with neonatal cardiomyocytes via a mechanism independent of histone deacetylase inhibition, Cell Transplant. 21 (2012) 985–996, https://doi.org/10.3727/096368911X593145.

[43] J.F. Heubach, E.M. Graf, J. Leutheuser, M. Bock, B. Balana, I. Zahanich, T. Christ, S. Boxberger, E. Wettwer, U. Ravens, Electrophysiological properties of human mesenchymal stem cells, J. Physiol. 554 (2004) 659–672, https://doi.org/10.1113/jphysiol.2003.055806.

[44] M.G. Chang, L. Tung, R.B. Sekar, C.Y. Chang, J. Cysyk, P. Dong, E. Marbán, M.R. Abraham, Proarrhythmic potential of mesenchymal stem cell transplantation revealed in an in vitro coculture model, Circulation 113 (2006) 1832–1841, https://doi.org/10.1161/CIRCULATIONAHA.105.593038.

[45] Y. Shiba, T. Gomibuchi, T. Seto, Y. Wada, H. Ichimura, Y. Tanaka, T. Ogasawara, K. Okada, N. Shiba, K. Sakamoto, D. Ido, T. Shiina, M. Ohkura, J. Nakai, N. Uno, Y. Kazuki, M. Oshimura, I. Minami, U. Ikeda, Allogeneic transplantation of iPS cell-derived cardiomyocytes regenerates primate hearts, Nature 538 (2016) 388–391, https://doi.org/10.1038/nature19815.

[46] V. Valiunas, G. Kanaporis, L. Valiuniene, C. Gordon, H.Z. Wang, L. Li, R.B. Robinson, M.R. Rosen, I.S. Cohen, P.R. Brink, Coupling an HCN2-expressing cell to a myocyte creates a two-cell pacing unit, J. Physiol. 587 (2009) 5211–5226, https://doi.org/10.1113/jphysiol.2009.180505.

[47] G.J. Brewer, C.W. Cotman, Survival and growth of hippocampal neurons in defined medium at low density: advantages of a sandwich culture technique or low oxygen, Brain Res. 494 (1989) 65–74.

[48] M.T. Mommersteeg, W.M. Hoogaars, O.W. Prall, C. de Gier-de Vries, C. Wiese, D.E. Clout, V.E. Papaioannou, N.A. Brown, R.P. Harvey, A.F. Moorman, V.M. Christoffels, Molecular pathway for the localized formation of the sinoatrial node, Circ. Res. 100 (2007) 354–362, https://doi.org/10.1161/01.RES.0000258019.74591.b3.

[49] C. Wiese, T. Grieskamp, R. Airik, M.T. Mommersteeg, A. Gardiwal, C. de Gier-de Vries, K. Schuster-Gossler, A.F. Moorman, A. Kispert, V.M. Christoffels, Formation of the sinus node head and differentiation of sinus node myocardium are independently regulated by Tbx18 and Tbx3, Circ. Res. 104 (2009) 388–397, https://doi.org/10.1161/CIRCRESAHA.108.187062.

[50] R.J. Blaschke, N.D. Hahurij, S. Kuijper, S. Just, L.J. Wisse, K. Deissler, T. Maxelon, K. Anastassiadis, J. Spitzer, S.E. Hardt, H. Schöler, H. Feitsma, W. Rottbauer, M. Blum, F. Meijlink, G. Rappold, A.C. Gittenberger-de Groot, Targeted mutation reveals essential functions of the homeodomain transcription factor Shox2 in sinoatrial and pacemaking development, Circulation 115 (2007) 1830–1838, https://doi.org/10.1161/CIRCULATIONAHA.106.637819.

[51] A.M.D. Végh, A.D. den Haan, L. Cócera Ortega, A.O. Verkerk, J.P.G. Sluijter, D. Bakker, S. van Amersfoorth, T.A.B. van Veen, M. Klerk, J. Seppen, J.M.T. de Bakker, V.M. Christoffels, D. Geerts, M.J.T.H. Goumans, H.L. Tan, G.J.J. Boink, Cardiomyocyte progenitor cells as a functional gene delivery vehicle for long-term biological pacing, Molecules 24 (2019), https://doi.org/10.3390/molecules24010181.

[52] G.J. Boink, A.O. Verkerk, S.C. van Amersfoorth, S.J. Tasseron, R. van der Rijt, D. Bakker, A.C. Linnenbank, J. van der Meulen, J.M. de Bakker, J. Seppen, H.L. Tan, Engineering physiologically controlled pacemaker cells with lentiviral HCN4 gene transfer, J. Gene Med. 10 (2008) 487–497, https://doi.org/10.1002/jgm.1172.

[53] M. Tong, X.J. Yang, B.Y. Geng, L.H. Han, Y.F. Zhou, X. Zhao, H.X. Li, Overexpression of connexin 45 in rat mesenchymal stem cells improves the function as cardiac biological pacemakers, Chin. Med. J. 123 (2010) 1571–1576.